DESIGNING A SPATIAL NAVIGATION PARADIGM FOR ANALYSING THE EFFECT OF MENTAL OVERLOAD ON MILD COGNITIVE IMPAIRMENT IN ALZHEIMER PATIENTS

A Thesis

submitted to
Indian Institute of Science Education and Research Pune in partial fulfilment of the requirements for the BS-MS Dual Degree Programme
by

SHREELEKHA B S

Indian Institute of Science Education and Research Pune
Dr. Homi Bhabha Road,
Pashan, Pune 411008, INDIA.
Date: March , 2024

Under the guidance of
Supervisor: Dr. Pragathi Priyadharsini Balasubramani,
Assistant Professor
From May 2023 to March 2024
INDIAN INSTITUTE OF TECHNOLOGY, KANPUR

Certificate

This is to certify that this dissertation entitled "**DESIGNING A SPATIAL NAVIGATION PARADIGM FOR ANALYSING THE EFFECT OF MENTAL OVERLOAD ON MILD COGNITIVE IMPAIRMENT IN ALZHEIMER PATIENTS**" towards the partial fulfilment of the BS-MS dual degree programme at the Indian Institute of Science Education and Research, Pune represents study/work carried out by **SHREELEKHA B S** at Indian Institute of Technology, Kanpur under the supervision of **Dr PRAGATHI PRIYADHARSHINI BALASUBRAMANI,** Assistant Professor, Department of Cognitive Science, during the academic year 2023-2024.

Dr. Pragathi Priyadharsini Balasubramani

Committee:
Dr. Pragathi Priyadharsini Balasubramani
Dr. Suhita Nadkarni

This thesis is dedicated to my sister and my parents

Declaration

I hereby declare that the matter embodied in the report entitled "**DESIGNING A SPATIAL NAVIGATION PARADIGM FOR ANALYSING THE EFFECT OF MENTAL OVERLOAD ON MILD COGNITIVE IMPAIRMENT IN ALZHEIMER PATIENTS**" are the results of the work carried out by me at the Department of Cognitive Science, Indian Institute of Technology (IIT) Kanpur , under the supervision of Dr Pragathi Priyadharsini Balasubramani, and the same has not been submitted elsewhere for any other degree. Wherever others contribute, every effort is made to indicate this clearly, with due reference to the literature and acknowledgement of collaborative research and discussions.

SHREELEKHA B S
20191032

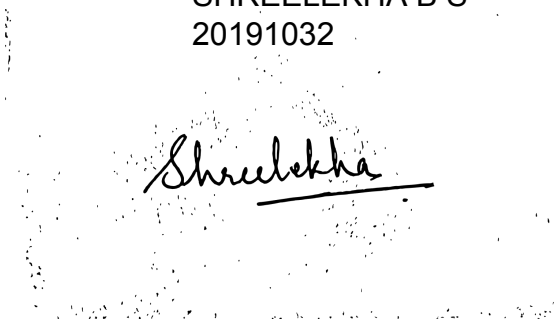

Table of Contents

List of Tables

List of Figures

Abstract

The research investigates the association between spatial navigation and mental overload among those with Mild Cognitive Impairment (MCI) and the inceptive stages of Alzheimer's disease (AD). Employing a multifaceted approach, it combines spatial navigation tasks with a digit numbering working memory challenge to induce mental overload. Electroencephalography (EEG) is utilized to study cognitive effects, particularly employing the Mismatched Negativity (MMN) task to identify states of mental overload and explore changes in cognitive resources allocation in response to auditory stimuli.

The central hypothesis posits that the degree of mental overload, reflected in spatial navigation performance, can signal cognitive deterioration during the MCI and early stages of Alzheimer's. The study intends to develop a framework for examining this hypothesis, establishing a system for objectively diagnosing AD during the MCI stage.

Three different design approaches, Virtual Reality and Physical world real time navigation paradigms were implemented with consistent modification and enhancement.

Analysis of the MMN task includes examining Event Related Potential peaks from EEG data, representing the brain's initial detection and processing of deviant stimuli and variation of these responses to be representative of resource distribution, respectively. Fz, Cz, and Pz signals are primarily used for event-related potentials, with each signifying different cognitive functions such as decision-making, spatial processing, and stress indication.

Insights from ERP analysis suggest that EEG post-processing and ERP derivation might be sensitive for real-time navigation paradigms. Further analysis will progress with Time Frequency Analysis of EEG data and enhanced data collection. Previous EEG investigations have consistently revealed neural changes in MCI and AD patients, including changes in alpha, beta, delta, and theta brainwave oscillations, decreased complexity and coherence in EEG recordings, as well as lower ratios of high alpha to low alpha and theta to gamma waves, proposed as potential biomarkers for early AD detection.

Acknowledgments

I would like to express my heartfelt gratitude to everyone who has contributed to the completion of this thesis.

First and foremost, I am immensely thankful to my supervisor,Dr. Pragathi Priyadharsini Balasubramani for her unwavering support, guidance, and motivation throughout this journey. I am also grateful to my expert , Dr Suhita Nadkarni . Their mentorship has been invaluable, and I am truly grateful for their belief in me.

I extend my deepest appreciation to Avinash sir for his constant input and collaboration, which enriched the depth and quality of my work.

I am indebted to my institute and the opportunities it has provided, particularly IIT Kanpur and the Cognitive Science Department, for their resources and facilities that have facilitated my research.

I owe a debt of gratitude to my parents and my sister for their unwavering support, encouragement, and understanding throughout this endeavor.

Special thanks are due to Prof. Klaus Gramann, Ayon Ghosh,Mr Hari Prakash Tiwari, Mr. Yangyulin Ai, and Mr. Amritmay Biswas for their support and insightful contributions to my project.

I am also grateful to my labmates at the Cognitive Science Department for their camaraderie and collaboration, which made this journey more enriching.

To all my friends, supporters, and well-wishers who have interacted with me, I extend my sincere thanks. Your encouragement and positivity have been a constant source of strength.

In conclusion, I am deeply thankful to each and every individual mentioned above, as well as those who may not be explicitly named but have contributed in various ways to my academic and personal growth. Thank you.

Contributions

Contributor name	Contributor role
Dr. Pragathi Priyadharsini Balasubramani, Dr Subasree Ramakrishnan, Shreelekha B S	Conceptualization Ideas
Prof Dr Klaus Gramann	Methodology
Dr Avinash K Singh, Ayon Ghosh	Software
	Validation
	Formal analysis
Mr. Hari Prakash Tiwari, Shreelekha B S	Investigation
IIT Kanpur, Translational Neuro Lab, Swaraj Vridha Ashram, Kanpur	Resources
	Data Curation
	Writing - original draft preparation
	Writing - review and editing
	Visualization
Dr. Pragathi Priyadharsini Balasubramani, Dr. Suhita Nadkarni	Supervision
	Project administration
IIT Kanpur, NeuroClinical Innovative Solutions Pvt Ltd	Funding acquisition

.

Chapter 1 Introduction

Alzheimer's disease (AD) is a neurodegenerative condition defined by the irreversible changes in the brain, commonly associated with dementia, denoting a decline in memory, cognitive faculties, and daily functioning. As highlighted in a 2019 report from Alzheimer's Disease International (ADI), worldwide, there are approximately 50 million instances of dementia, and an additional 10 million new cases emerge annually. Advanced age is identified as the main risk factor, with the majority of Alzheimer's diagnosis manifesting in individuals aged 65 and older. At the molecular level, AD is found to be the buildup of beta-amyloid peptide deposits and extra phosphorylated Tau protein. (McKhann *et al.*, 2011)

MOLECULAR EXPLORATION

In the molecular exploration and cellular level, during the early phases of AD, changes in baseline connectivity are noticed, marked by a decline in posterior regions of the Default Mode Network (DMN) juxtaposed with a rise in ventral and anterior DMN networks, a critical interconnected brain network integral to consciousness and cognitive function (Damoiseaux *et al.*, 2012). As AD progresses, functional connectivity diminishes across all regions of the DMN. The pathology of AD initially targets anterior medial temporal lobe structures, with histopathological changes manifesting initially affecting the entorhinal cortex and hippocampus, the pathology progresses to involve the temporal pole, parahippocampal gyrus, middle temporal gyri and inferior during mild cognitive impairment (MCI) and preclinical AD ((Petersen *et al.*, 2006; Braak and Braak, 1995). In alignment with this neuropathological advancement, rapid atrophy is observed in the perirhinal cortices and entorhinal as well as the hippocampus during the initial phases of MCI and AD (Schmidt-Wilcke *et al.*, 2009; Pennanen *et al.*, 2004; Risacher *et al.*, 2010).

Additionally, reduced metabolism is noted in these areas, and even cognitively normal individuals who later develop MCI show signs of anteromedial temporal atrophy (Smith *et al.*, 2007). Further stages of AD are distinguished by the atrophy of the parahippocampal cortex and fusiform gyrus (McDonald *et al.*, 2009; Karow *et al.*, 2010).

Several neuroimaging investigations have revealed significant metabolic and structural alterations in the parietal lobe in the early stages of AD. Studies have reported cortical atrophy in the inferior parietal lobule and precuneus during the initial

stages of MCI, with volume reduction in these areas consistently observed in individuals progressing from MCI to AD (Whitwell *et al.*, 2008; Karas *et al.*, 2008). Furthermore, such atrophy has been noted even in individuals initially classified as cognitively normal who later develop MCI and AD (Smith *et al.*, 2007; Jacobs *et al.*, 2011); Smith *et al.*, 2007). Increased metabolism has also been detected in the inferior and superior parietal lobules among MCI patients, particularly in those who later convert to AD Nobili *et al.*, 2008;). In the cingulate gyrus, early involvement of the retrosplenial cortex (RSC) and posterior cingulate has been seen in AD progression, with atrophy and hypometabolism evident in mild AD and early MCI stagesChételat *et al.*, 2002;). Severely increased metabolism in the posterior cingulate cortex is descriptive of incipient AD and is detectable even in MCI patients Pappatà *et al.*, 2010;). Conversely, changes in the frontal cortex due to diseased conditions in the nervous system occur later in the AD course, with hypometabolism and atrophy becoming prominent in the prefrontal cortex during the late phases of MCI and in individuals who later develops AD ((Drzezga *et al.*, 2003); McDonald *et al.*, 2009).

PROGRESSION AND DIAGNOSIS OF ALZHEIMER's

Alzheimer's disease progresses through well-defined stages, each marked by distinct symptoms and changes in cognitive and functional capabilities. Although the rate of progression varies among individuals, there are significant and commonly acknowledged stages such as the preclinical stage and MCI along with different stages of AD ranging from mild to severe.

During the preclinical stage, individuals may not manifest overt cognitive symptoms, yet underlying changes are occurring within the brain, such as the build-up of plaques of beta-amyloid and twisted fibers of tau protein. Biomarkers, detectable through imaging or cerebrospinal fluid analysis, may indicate the presence of pathology associated with AD.

The onset of MCI due to AD is depicted by the subtle changes in memory, language, or other cognitive functions, noticeable to the individual or close relatives but not significantly impairing day to day activities. Some individuals with MCI may progress to Alzheimer's disease, whereas others may stay stable or sometimes even go back to performing normal cognitive functions.

As Alzheimer's disease advances, cognitive decline gradually impedes daily functioning. In the mild stage, individuals struggle with recalling recent events,

navigating familiar environments, managing finances or medications, and solving problems. Mood disturbances, such as depression or anxiety, may also emerge. Progressing to the moderate stage, cognitive deterioration intensifies, significantly impairing independent activities. Memory loss worsens, communication becomes increasingly challenging, and behavioral disturbances, like agitation or aggression, may arise. Ultimately, in the severe stage, individuals experience profound cognitive and functional impairment, necessitating comprehensive assistance for daily tasks. Memory impairment reaches a severe degree, communication abilities decline substantially, and motor function may deteriorate, leading to difficulties with mobility and bodily functions.

Mild Cognitive Impairment (MCI) marks the initial phase of AD, depicted by cognitive decline and memory loss while maintaining functional independence. MCI outcomes vary, with some individuals experiencing a return to normal cognition or stability. Clinicians classify MCI based on specific cognitive impairments: Amnestic MCI primarily affects memory, while Nonamnestic MCI impacts problem-solving and task completion. Despite being less severe than Alzheimer's, MCI symptoms include forgetfulness, missed events, and difficulty with verbal expression.

We were mainly interested in the MCI stage of AD because it is present right after Preclinical stage of Alzheimer's which shows highest promise for any intervention of cure and diagnosing it at that stage will help us with a chance to pause it from progressing drastically and differentiate it between other neurodegenerative diseases which share dementia as a progressive symptom. Right now available diagnosing of Alzheimer's has been mostly subjective tests, and self reports that are all in the hands of the patient. Clinical diagnosable measures include invasive techniques such as magnetic resonance imaging and computed tomography scans and Positron emission tomography scans. Cerebrospinal fluid (CSF) analysis involves collecting CSF via a spinal tap and measuring proteins associated with Alzheimer's, but these cannot be implemented to diagnose Alzheimer’s in the pre-clinical stage and MCI stage nor able to have any intervention at this diagnosis stage.

Thus, there exists a necessity for non-invasive diagnostic methods. In this regard, Electroencephalography (EEG) presents itself as a viable option due to its non-invasiveness, easy to carry around and cheaper cost. This technique directly measures and record brain activity with sufficient time resolution, making it a promising tool for finding neural biomarkers associated with MCI and AD (Vecchio *et*

al., 2020; Meghdadi *et al.*, 2021; Vecchio *et al.*, 2018; Smailovic *et al.*, 2021). Various studies have provided evidence supporting the use of EEG to differentiate between MCI and AD patients among healthy individuals albeit with varying degrees of sensitivity and specificity (Farina *et al.*, 2020). Previous EEG research involving both MCI and AD patients has consistently revealed changes in the neural activity patterns compared to healthy cohorts, including increased delta and theta oscillations and reduced alpha and beta rhythm activity. These alterations are considered great neural biomarkers for initial stage AD detection due to their strong correlative power with cognitive function in patients (Cassani *et al.*, 2017; Musaeus *et al.*, 2018; Farina *et al.*, 2020; Hatz *et al.*, 2015; Monllor *et al.*, 2021).

Alzheimer's patients commonly encounter challenges in remembering and retrieving memories. A significant obstacle in memory retrieval is the competition between relevant and irrelevant information, particularly when such information shares contextual, semantic, or emotional features. In the absence of mechanisms that are effective enough to mitigate the competition, individuals might struggle to recall the intended incidents due to the interference of irrelevant information. Fortunately, inhibitory mechanisms play a crucial role in preventing such failures by suppressing competition during memory retrieval (Bjork and Bjork, 1996). Retrieval inhibition, which involves the capabilities to mask irrelevant and unwanted information during recall, and is seen to be compromised with aging. May and Hasher (May and Hasher, 1998) suggest that adults at very old age experience challenges in inhibiting the activation of unwanted stimuli and thoughts. Consequently, as task-irrelevant information floods their memory, there are fewer resources available for processing task-relevant information, thereby contributing to cognitive decline..

Our research focuses on the exacerbating impact of stress on dementia, particularly in the MCI stage, where the choking effect or mental overload significantly worsens this condition. Our specific focus lies in utilizing Mismatched Negativity (MMN) as a marker for identifying stress levels in this context.

MISMATCHED NEGATIVITY

Event-related potential (ERP) recordings have become increasingly utilized in evaluating cognitive abilities and information processing in individuals with Rett syndrome (RTT) as well as in animal models. This approach provides quantitative insights into brain function, including cortical network dynamics, without solely depending on observable behavioral responses. In particular, the mismatch

negativity (MMN) component of ERPs enables the examination of early auditory processing, auditory discrimination, and sensory memory without necessitating active involvement from the participant (Brima *et al.*, 2019).

MMN, as an ERP response, reflects the brain's automatic detection of discernible changes within a continuous auditory stimulus stream. These changes can encompass abstract alterations, such as deviations from established patterns or rules derived from recent auditory input. The ability of MMN to detect violations of abstract sequential patterns suggests a connection between automatic cognitive processes and higher-order functions within the auditory cortex. This implies the existence of a rudimentary form of sensory intelligence, wherein complex auditory analyses occur beyond conscious perception. MMN serves as a crucial tool for elucidating intricate auditory processing mechanisms (Brima *et al.*, 2019).

To comprehend the role of MMN within the broader framework of organism functioning, it is crucial to consider the tasks undertaken by the auditory sensory system to generate neural representations of environmental sound sources effectively. Firstly, the system must encode stimulus inputs, creating memory traces that capture the original sources and the derived regularities. Secondly, it must continuously update these representations to ensure the ongoing integrity of sound sources. Recent hypotheses propose that the processes reflected by MMN entail anticipation of forthcoming representations of immediate future stimuli. This sensory updating process is suggested to have privileged access to frontal attentional control mechanisms, facilitating rapid involuntary attentional shifts towards stimulus changes. The growing popularity of MMN in cognitive neuroscience research stems from its utility in examining listeners' processing of complex auditory scenes, speech discrimination concerning categorical perception, and native-language experience. These advancements underscore the versatility of MMN as a tool for diverse scientific and clinical applications. In clinical settings, MMN's passive elicitation allows for the examination of complex brain functions in individuals with behavioral and cognitive impairments, offering an objective functional measure of cortical processing (Näätänen *et al.*, 2014).

SPATIAL NAVIGATION

Spatial disorientation represents an early indicator of AD, alongside the commonly recognized disabilities related to memory. In recent years, there has been notable expansion in research concerning spatial impairments associated with this neurodegenerative disorder. It is plausible that diminishing spatial navigation skills could emerge as an additional diagnostic indicator for AD. However, Spatial navigation is a multifaceted ability. The capability of creation and sustaining routes between different locations involves various spatial strategies that activate different brain regions. Numerous studies in the past two decades have delved into visuo-spatial deficits in MCI and AD. The dominant viewpoint regarding these impairments can be generally divided into two main approaches: one group of research emphasizes the disorientation due to visuo-perceptual, and its connection with visual-spatial attention and optic flow perception. In contrast, another set emphasizes deficits in cognitive mapping in these patients, particularly regarding their use of allocentric navigation. Moreover, Some studies suggest a possible link between spatial disorientation in individuals with AD and MCI. and the functioning of both the parietal and medial temporal lobes. Recent reviews in this subject either support the allocentric perspective, suggest integrating visuo-perceptual factors and cognitive mapping, or promote a multifocal theory of disease progression ranging from lateral to frontal and temporal to parietal brain regions, accompanied by related cognitive impairments.

The role of the hippocampus has been documented in many allocentric navigation studies that involves the importance of hippocampus in spatial deficits in MCI and AD: disruptions in spatial navigation within the Morris water maze, known as the Blue Velvet Arena (BVA), have been observed in individuals with Alzheimer's disease (AD). In the same setup, the AD group with more defined symptoms faced challenges navigating using both hometown and wall cues, whereas the amnestic single-domain MCI group showed impairment only in tasks involving allocentric cues (Hort *et al.*, 2007), indicating a peculiar deficiency indicates the hippocampus. Patients with AD also had difficulty navigating in a maze created in virtual reality arena using a map, that required the translation of the allocentric view on the map to the maze in egocentric direction (Morganti, Stefanini and Riva, 2013). Egocentric memory enables the recollection of one's spatial position in relation to one's own location and orientation in space. Structures in the inferior and superior parietal lobes

showed increased activity during various egocentric tasks, as seen in the Morris water maze, Virtual City; (Parslow et al., 2004; (Wolbers, Weiller and Büchel, 2004) as well as in an environment without characteristic objects (Wolbers *et al.*, 2008). Egocentric navigation is deteriorated in patients with MCI and AD as shown by two types of experiments. In both physical and virtual versions of the Morris water maze, individuals with amnestic Mild Cognitive Impairment (MCI) and non-memory-related disorders exhibit behaviors akin to those of Alzheimer's disease (AD) patients when searching for a concealed target solely based on their initial position (Hort *et al.*, 2007). In a virtual reality maze where participants were instructed to rely solely on sequences of egocentric turns for navigation, individuals with amnestic MCI struggled to learn the route to a concealed reward (Weniger *et al.*, 2011).

There are few major reasons for using spatial navigation task in order to assess for AD.

Impairments in spatial navigation have the ability to reveal underlying pathophysiological changes in preclinical AD. Variations and defects in spatial navigation can predict AD at the pre-clinical stage itself, including any pathophysiological implications.

The brain regions most impacted at the onset of AD pathology are crucial nodes within the spatial navigation system.

Individuals at genetic risk exhibit modified spatial navigation patterns prior to the onset of any symptoms related to episodic memory.

Even before onset of any Alzheimer symptoms, especially related to dementia or episodic memory, one can observe effect on spatial navigation

Spatial navigation is increasingly recognized to be feasible and economical marker for research on detecting AD,offering significant implications for future diagnostic and treatment strategies.

One of the navigation tasks employed involves customizing the operation of a virtual supermarket. Known as the Virtual Supermarket Test (VST), this spatial navigation assessment evaluates egocentric orientation, allocentric orientation, and translational direction knowledge. This test was selected due to its prior use in research, where it demonstrated navigation deficits in AD patients. Our aim was to investigate whether patients' performance on this test correlates with their levels of social and spatial disorientation. (Tu *et al.*, 2015; Tu *et al.*, 2017; Lowry *et al.*, 2020).

VST is considered to provide significant results with low immersion and high predictability between various populations, suggesting that VST is useful and acceptable to the target population.

THESIS AIM

Our research investigates the connection between spatial navigation and mental overload in individuals with Mild cognitive impairment (MCI) and initial-stage Alzheimer's disease. We employ a multifaceted approach that combines spatial navigation tasks with a digit numbering working memory challenge to induce mental overload.

Our research relies on electroencephalography (EEG) to study the cognitive effects of mental overload. We use the Mismatched Negativity (MMN) task to identify states of mental overload, exploring how cognitive resources and attention allocation change in response to auditory stimuli. Mismatch Negativity (MMN), an event-related potential indicative of fundamental pre-attentive cognitive mechanisms. Our central hypothesis suggests that the degree of mental overload, as reflected in spatial navigation performance, is indicative of cognitive decline in MCI and early Alzheimer's stages. We posit that more significant mental overload corresponds to pronounced cognitive impairment, especially in spatial navigation.

In this Thesis, we aim to design a paradigm involving the above features to test our hypothesis. This aims to provide a translational set up to objectively diagnose Alzheimer’s disease at the Mild Cognitive Impairment Stage.

Chapter 2 **Materials and Methods**

APPROACH 1

Approach 1 encompassed the development of a virtual reality (VR) navigation paradigm known as the WALK project, pioneered by Dr. Avinash K Singh from the University of Technology Sydney, Australia. It was designed on VR gaming interface, Unity Hub 3.4.2 version. The VR headset used was VIVE Pro 2, designed along with Basestation 2.0 and two Controllers (2018 version) and along with a treadmill mounting kit. It was equipped with a 120-degree field of view and StreamVR 1.0 and 2.0 version VR streaming. The navigational task within this paradigm involved a 4-5 minute exploration of a cityscape featuring a singular curve, challenging participants' spatial awareness and orientation abilities. Upon completion, participants were queried on the homing direction, representing the angular direction from the final position to the initial point of navigation. The accuracy of this homing direction was calculated along with the response time for each trail.

This approach faced suffered several limitations

- The movement is not adapted accordingly as the head motion. This would act as a confound during motion on the hovering treadmill implementation. It did not provide an independent motion irrespective of the head placement and users vision.
- The Apparatus (VR headset and controller) did not prove to be adaptable or suitable for our target population(Age >65). An appropriate experimentation time is 20 minutes, and the average of 5 trails incorporated in a single experiment time would be insufficient. Additionally, other physiological side effects were observed , like head-heaviness, discomfort to eyes and headache occurring due to long exposure to VR proved it difficult to continue the experiment using virtual reality.

Fig 2.01, : VR Set up used. An approximate area of 6 feet X 4 feet is calibrated for movement space for VR game set up.

Fig 2.02 : VR Game set up. Figure on the left is the prompt to question the homing direction. Fig 2.02 right : VR game set up to imitate real settings.

APPROACH 2

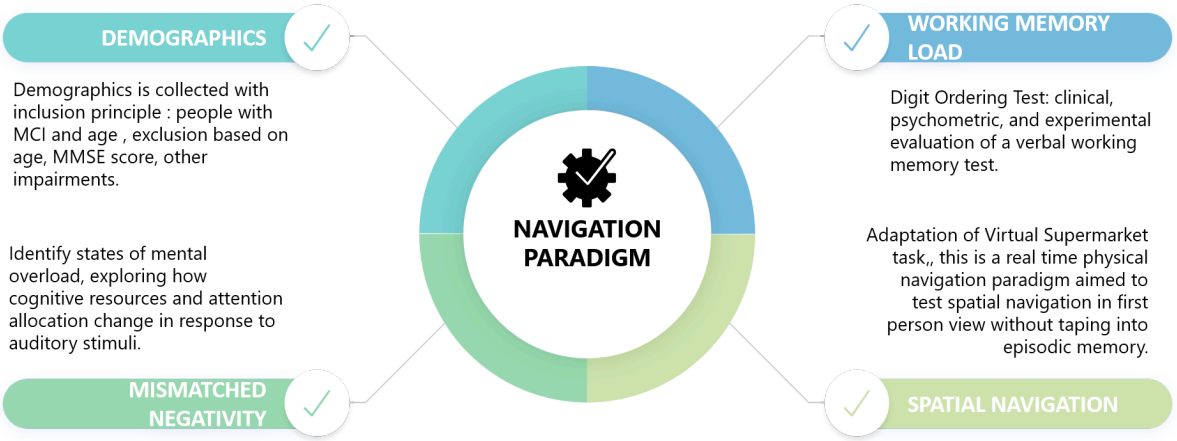

Fig 2.03 : 4 Domains involved in Physical World Navigation Paradigm

SPATIAL NAVIGATION

The Virtual Supermarket, an application that is Dutch-developed, offers a three-dimensional software interface replicating the experience of shopping in a real supermarket (Waterlander *et al.*, 2011). It includes an assessment of spatial orientation conducted within a virtual environment resembling a real-world supermarket. Notably, the virtual environment lacks distinctive landmarks, requiring participants to encode spatial information incidentally during test trials.

In the described paradigm's English version, participants watch videos from a first-person perspective as they navigate predefined locations within the virtual market. This navigation involves a series of 90° turns while imagining themselves pushing a shopping trolley to various destinations within the supermarket. After every trial, subjects were asked to identify the direction in which the initial starting point was (referred to as the "homing direction"). It's important to note that all trials begin from the same starting point but follow varying paths to different destinations. To maintain consistency, the length and number of turns in each trial segment are standardized. Crucially, participants do not receive any feedback during the testing trials (Tu *et al.*, 2015).

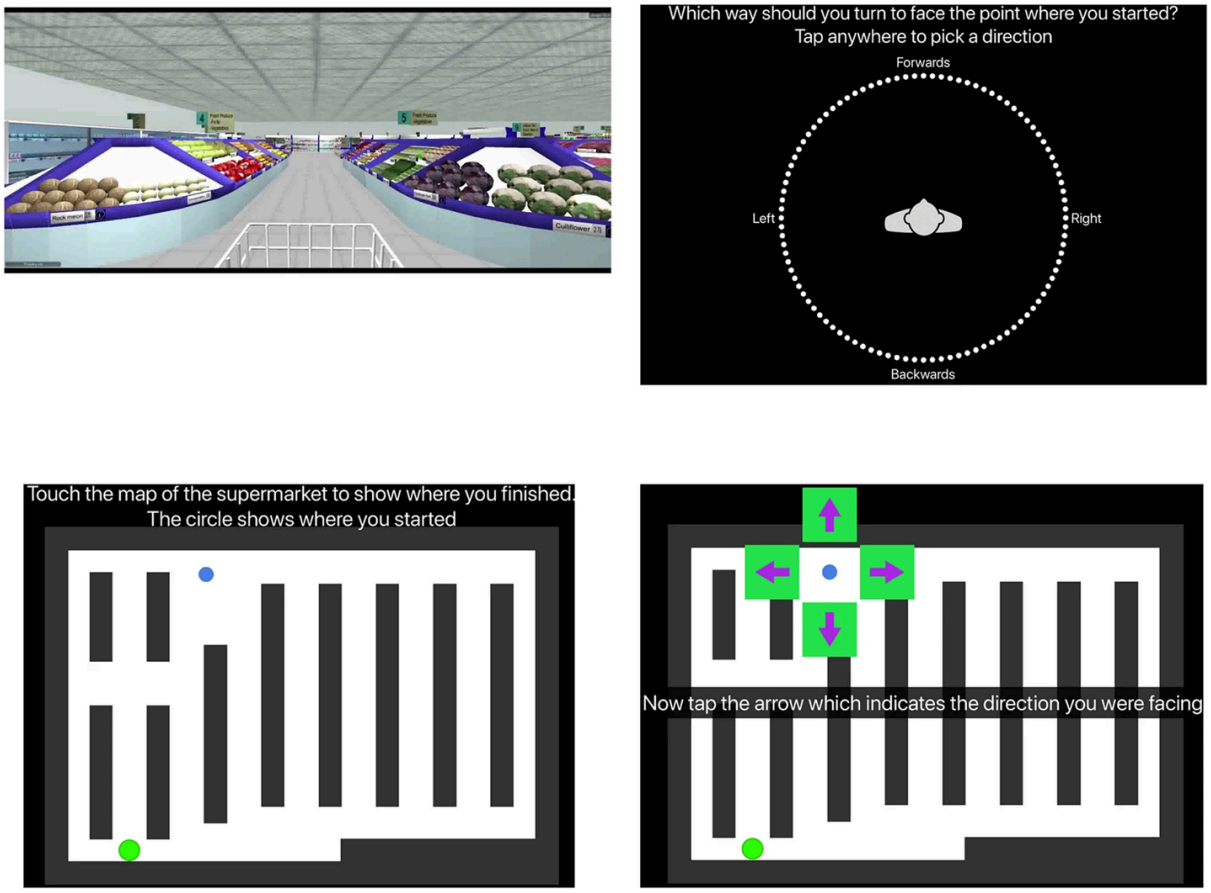

Fig 2.04: Credits: (Puthusseryppady *et al.*, 2022) It depicts the measures implemented in the Virtual SuperMarket Task. Participants are evaluated on Egocentric and Allocentric navigation questions. Figure depicts the game setup, homing angle question, homing direction question and Allocentric orientation evaluation respectively.

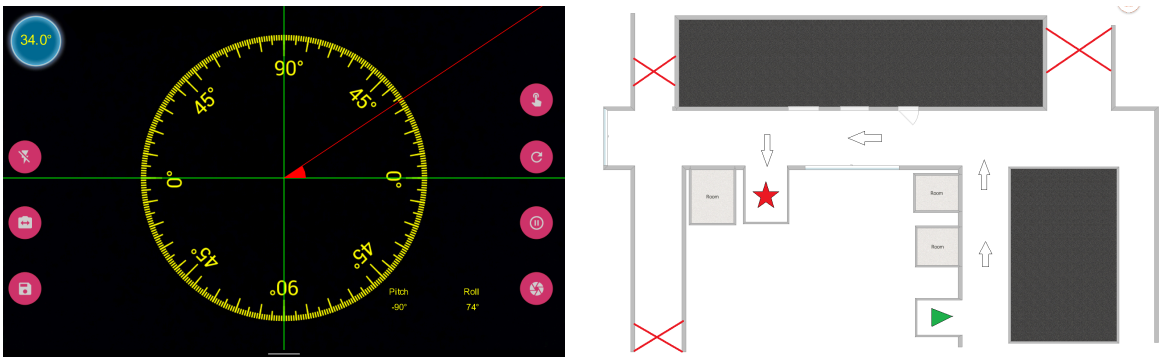

Fig 2.05: (a)Laser level meter used for obtaining the homing direction. This is calibrated for the specific orientation set up of each target location and also records information on inclination, pitch and roll if required to calibrate. (b) Bird eye view of the navigation paradigm

map. Initial orientation and position is marked along with the target position and an ideal path direction

The adapted paradigm mirrors real-world scenarios within an indoor building environment featuring identical rooms and passages. Navigation comprises four trials wherein rooms serve as destinations, involving a standardized single 90-degree turn from the starting point. Designations include the "Home Position" for the initial room and "Target Positions" for subsequent destinations, organized in a circuit whereby the previous trial's Target Position becomes the next trial's Home Position. Following each trial, participants must identify the direction of the Home Position (referred to as the "homing direction"). These trials encompass two levels of complexity, characterized by obtuse or acute homing angles.

Prior to testing, participants receive instructions detailing a bird's-eye view map displaying Target Positions, orientation, and optimal pathways. They are shown in the map as an illustration of optimal movement to different building locations. Upon reaching the Target Position, participants must determine the homing direction. They are informed about starting from various locations across trials and are instructed to remember the starting direction after each trial. At trial completion, participants utilize a digital 360-degree protractor, featuring a movable arm, and are prompted with a query ("The previous location, Target Location No, is situated in which direction?") to obtain an answer by positioning the protractor hand to selected angle. This protractor, calibrated based on participant position in the room and considering azimuth bearing pitch and roll, measures the angle using an Android App named Angle Meter, employing a laser level for precise angle measurement.

MISMATCHED NEGATIVITY

The oddball paradigm is a frequently employed experimental methodology within cognitive neuroscience and psychology, designed to assess the brain's response to novel or unexpected stimuli. This involves showing participants a series of repetitive "standard" stimuli interrupted by occasional "deviant" stimuli. The goal is to trigger automatic responses that reflect the brain's capacity to detect and process novel events. In this auditory paradigm, standard tones (constituting 80 percent of the stimuli) are randomly intermixed with deviant tones (comprising 20 percent). These tones are characterized by a 1000 Hz frequency, with a rise time and fall time of

10ms. The standard tones last for 100ms, whereas the deviant tones endure for 180ms. These stimuli are presented with stimulus onset asynchronies (SOAs) of 450ms and an inter-tap interval (ITI) of 900ms.

The ITI denotes the duration between the cessation of one stimulus (either standard or deviant) and the onset of the subsequent stimulus in the sequence. It signifies the interval during which no auditory stimuli are presented, while the SOA pertains to the temporal relationship between the initiation of different stimuli within the sequence.

Furthermore, a standard oddball Mismatched Negativity Task is utilized as a marker to gauge mental overload. Baseline EEG recordings of participants are obtained during two conditions: (a) Rested with eyes open, and (b) Rested with eyes closed. The experimental setup adheres to the aforementioned specifications, with standard tones lasting 100ms and deviant tones extending to 180ms, both featuring a frequency of 1000Hz.

DEMOGRAPHICS

The Hindi Mental Status Examination (HMSE) serves as a valuable tool for evaluating cognitive ability. Comprising 20 distinct test components, the HMSE scrutinizes various cognitive domains including orientation, attention, recall, naming, repetition, comprehension, adherence to commands, sentence formulation, and visual perception. Each component yields a score, culminating in a total potential score of 30 points for the assessment

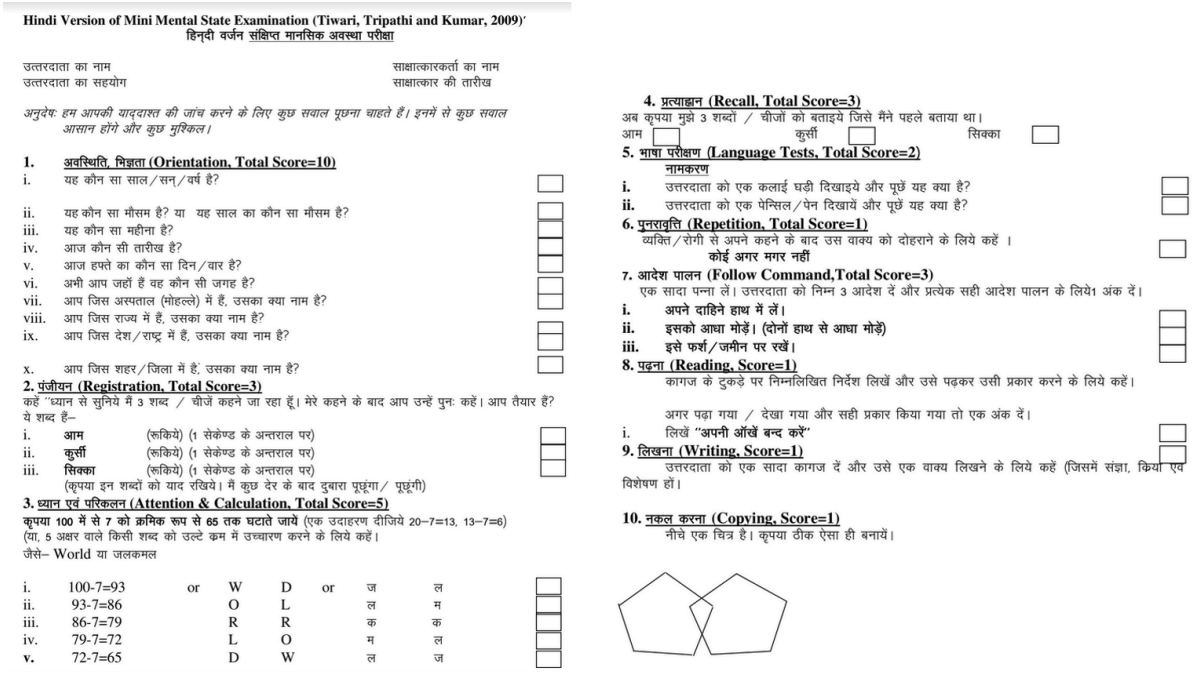

Hindi Version of Mini Mental State Examination (Tiwari, Tripathi and Kumar, 2009)'
हिन्दी वर्जन संक्षिप्त मानसिक अवस्था परीक्षा

उत्तरदाता का नाम — साक्षात्कारकर्ता का नाम
उत्तरदाता का सहयोग — साक्षात्कार की तारीख

अनुदेश: हम आपकी याद्दाश्त की जांच करने के लिए कुछ सवाल पूछना चाहते हैं। इनमें से कुछ सवाल आसान होंगे और कुछ मुश्किल।

1. अवस्थिति, भिज्ञता (Orientation, Total Score=10)
i. यह कौन सा साल/सन्/वर्ष है?
ii. यह कौन सा मौसम है? या यह साल का कौन सा मौसम है?
iii. यह कौन सा महीना है?
iv. आज कौन सी तारीख है?
v. आज हफ्ते का कौन सा दिन/वार है?
vi. अभी आप जहाँ हैं वह कौन सी जगह है?
vii. आप जिस अस्पताल (मोहल्ले) में हैं, उसका क्या नाम है?
viii. आप जिस राज्य में हैं, उसका क्या नाम है?
ix. आप जिस देश/राष्ट्र में हैं, उसका क्या नाम है?
x. आप जिस शहर/जिला में है, उसका क्या नाम है?

2. पंजीयन (Registration, Total Score=3)
कहें "ध्यान से सुनिये मैं 3 शब्द / चीजें कहने जा रहा हूँ। मेरे कहने के बाद आप उन्हें पुनः कहें। आप तैयार हैं? ये शब्द हैं–
i. **आम** (रूकिये) (1 सेकेण्ड के अन्तराल पर)
ii. **कुर्सी** (रूकिये) (1 सेकेण्ड के अन्तराल पर)
iii. **सिक्का** (रूकिये) (1 सेकेण्ड के अन्तराल पर)
(कृपया इन शब्दों को याद रखिये। मैं कुछ देर के बाद दुबारा पूछूंगा/ पूछूंगी)

3. ध्यान एवं परिकलन (Attention & Calculation, Total Score=5)
कृपया 100 में से 7 को क्रमिक रूप से 65 तक घटाते जायें (एक उदाहरण दीजिये 20–7=13, 13–7=6)
(या, 5 अक्षर वाले किसी शब्द को उल्टे कम में उच्चारण करने के लिये कहें।
जैसे– World या जलकमल

i.	100-7=93	or	W	D	or	ज	ल
ii.	93-7=86		O	L		ल	म
iii.	86-7=79		R	R		क	क
iv.	79-7=72		L	O		म	ल
v.	72-7=65		D	W		ल	ज

4. प्रत्याह्वान (Recall, Total Score=3)
अब कृपया मुझे 3 शब्दों / चीजों को बताइये जिसे मैंने पहले बताया था।
आम ☐ कुर्सी ☐ सिक्का ☐

5. भाषा परीक्षण (Language Tests, Total Score=2)
नामकरण
i. उत्तरदाता को एक कलाई घड़ी दिखाइये और पूछें यह क्या है?
ii. उत्तरदाता को एक पेन्सिल/पेन दिखायें और पूछें यह क्या है?

6. पुनरावृत्ति (Repetition, Total Score=1)
व्यक्ति/रोगी से अपने कहने के बाद उस वाक्य को दोहराने के लिये कहें ।
कोई अगर मगर नहीं

7. आदेश पालन (Follow Command,Total Score=3)
एक सादा पन्ना लें। उत्तरदाता को निम्न 3 आदेश दें और प्रत्येक सही आदेश पालन के लिये1 अंक दें।
i. अपने दाहिने हाथ में लें।
ii. इसको आधा मोड़ें। (दोनों हाथ से आधा मोड़ें)
iii. इसे फर्श/जमीन पर रखें।

8. पढ़ना (Reading, Score=1)
कागज के टुकड़े पर निम्नलिखित निर्देश लिखें और उसे पढ़कर उसी प्रकार करने के लिये कहें।
अगर पढ़ा गया / देखा गया और सही प्रकार किया गया तो एक अंक दें।
i. लिखें **"अपनी आँखें बन्द करें"**

9. लिखना (Writing, Score=1)
उत्तरदाता को एक सादा कागज दें और उसे एक वाक्य लिखने के लिये कहें (जिसमें संज्ञा, क्रिया एवं विशेषण हों।

10. नकल करना (Copying, Score=1)
नीचे एक चित्र है। कृपया ठीक ऐसा ही बनायें।

Fig 2.06: HMSE, a questionnaire to evaluate cognitive ability. Hindi adaptation of the MMSE Test

A demographics questionnaire is formulated for inclusions and exclusion for this study. Exclusion criteria is anyone scoring less than or equal to 17 (or Dementia stage) or in suffering from Dementia or any neurodegenerative disease.

Information on the following things are collected.

- Name age
- Blood group
- Alcohol, smoking involvement
- Pulmonary diseases
- Diabetes, Blood pressure, Cholesterol
- Other cardiovascular diseases
- Arthritis
- Stroke and epilepsy
- Hearing problems or aids
- Any significant medications

WORKLOAD PROFILE

The Workload Profile (Tsang & Velazquez, 1996) asks the subjects to provide the proportion of attentional resources used after they had experienced all of the tasks to be rated.. Subjects have available to them the definition of each question at the time of the rating.

Our questionnaire consists of 8 questions pertaining to each of this domain, as they are a major field of interest in our study, as well as 1 confidence question.

Each of these questions is scored from 1(least difficult / most confident) to 4(most difficult/ least confident). Workload Profile is usually measured as binary (0,1) allocation for each task based on the 8 sub domain categorization like the standard workload profile categorization where the binary is determined by 2 point threshold in the scale provided. Here we use the Or the standard 4 point involvement scale (Likert scale).In essence, a Likert scale is a means of expressing people's attitudes and thoughts on a subject or issue. A Likert scale is a type of psychometric scale that is frequently used in research to gauge participants' attitudes and opinions about a subject or issue. It makes use of questionnaires, which are frequently employed in place of rating scales. In simple terms, a 4-point Likert scale is a constrained Likert scale. The ratings on the individual dimensions are later summed for each task to provide an overall workload rating.

QUESTION
How easy or difficult was it to understand the task instructions? कार्य निर्देशों को समझना कितना आसान या कठिन था?
Was dealing with location and direction in the task mentally hard for you? क्या कार्य में स्थान और दिशा से निपटना आपके लिए मानसिक रूप से कठिन था?
How much effort did you need to understand what was spoken in the task? कार्य में जो बोला गया उसे समझने में आपको कितना प्रयास करना पड़ा?
Did you experience any mental difficulty when mentally visualizing task elements? क्या आपने कार्य तत्वों की मानसिक रूप से कल्पना करते समय किसी मानसिक कठिनाई का अनुभव किया?
Did you experience any mental effort or challenges while talking to people in the task? क्या आपने कार्य में लोगों से बात करते समय किसी मानसिक प्रयास या चुनौतियों का अनुभव किया?
Did the auditory information/ sound take your attention or disturb you during this trial? क्या इस परीक्षण के दौरान श्रवण संबंधी जानकारी/ध्वनि ने आपका ध्यान खींचा या आपको परेशान किया?
How easy or difficult was it to do the physical actions instructed in the task? कार्य में निर्देशित शारीरिक क्रियाओं को करना कितना आसान या कठिन था?
How confident are you with the answers provided by you to these questions? इन प्रश्नों के आपके द्वारा दिए गए उत्तरों को लेकर आप कितने आश्वस्त हैं?

Fig 2.07: Workload Profile Questionnaire used in the study.8 questions pertaining to each domain of analysis and 1 confidence question(in the last)

WORKING MEMORY

Working Memory Task implemented is Digit numbering Task (DNT) which is a standard verbal working memory where the participant has to memorize the sequence of numbers presented on the screen/ or voice, one at a time and recall to utmost accuracy usually recited as the same sequence or in ascending order. Before every navigation circuit, a sequence of numbers are presented which the participant has to recollect after the circuit, at the target location. Here the two complexities of working memory tasks used were Easy and Difficult , which is determined by

baselining done on each participant. The baselining is conducted in 2 blocks. FIrst block spans sequence of numbers from length 1 to n, where the participant attains zero percent accurate recall percentage for the third time. There are 3 trials for each length of sequence and accuracy percentage is calculated. Second block continues from the first block which spans the sequence length of numbers between 100 percent accuracy to zero percent. The 'Easy' sequence of length is considered to be the ceiling of 100 percent accuracy, and the 'Difficult' length to be the flooring, before zero percent accuracy is reached. The sequences are either verbally presented or visually, and is kept as a standard throughout the experiment to remove any confounds related to dependence on sensory perception. The standard rate of presenting seven digits within 5 seconds was validated as the most effective for identifying deficits in verbal working memory (Hoppe *et al.*, 2000). This result is adapted here to incorporate age variations and enable target population.

Digit numbering baselining standardization was done on three healthy participants(age ground between 23 and 29 years old) with the same block system described above.

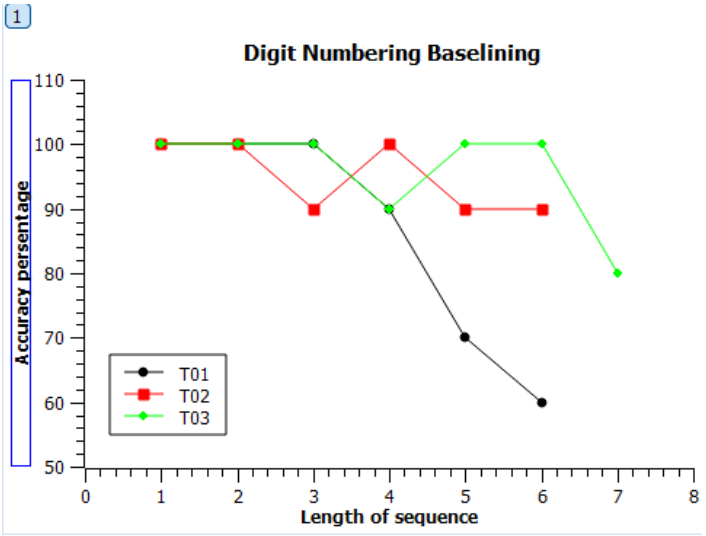

Fig 2.08: In this Digit numbering difficulty baselining, Each length of sequence was provided over 10 trials and the accuracy of recital was recorded over the three participants T01, T02, T03., in a standard Digit Span Task narration. Apart from T01, we do not see a reliable psychometric curve to accurately target difficult and easy levels for the participant. Continuing the trial, Easy(E)/ Difficult(D) was categorized as a mark of 100 percent accuracy just before a drop in performance and the length of sequence just before mental overload (accuracy < 50 percent) respectively. In format of (E/D) for each participant , for T01(3/6), T02(2,6), T03(4,7)

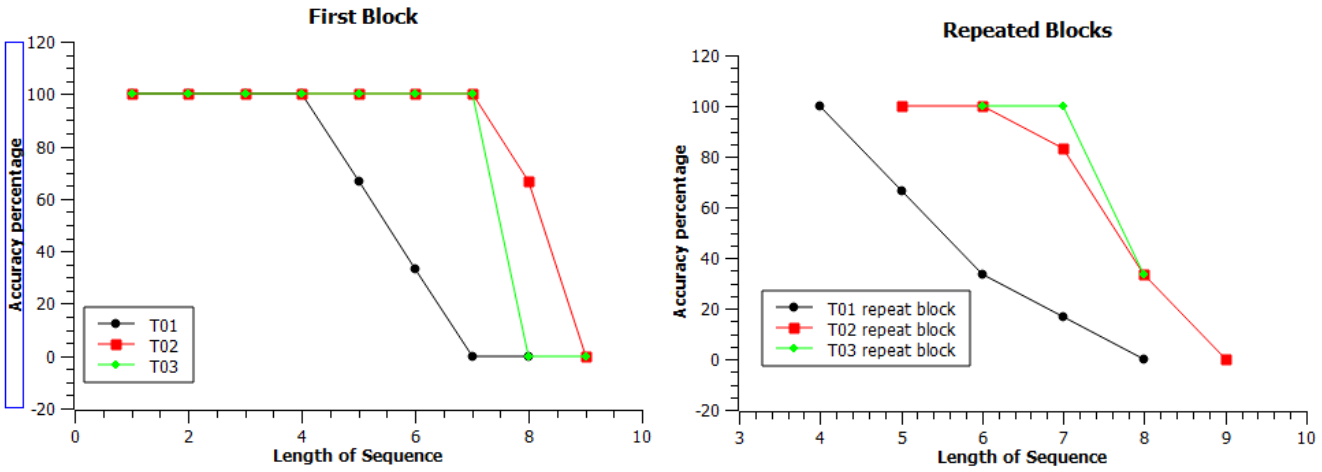

Fig 2.09: (a) First Block represents the first spanning across all lengths of sequences, with 3 trials for each length until the participant reaches 0 percent of accuracy. (b) Repeated blocks is additional 3 trials for thresholds(discontinuity) observed in First Block and the accuracy is calculated over all 6 trials. From this method of baselining we get T01 : (4, 5) T02 : (6, 7) T03 : (7,8)

PIPELINE

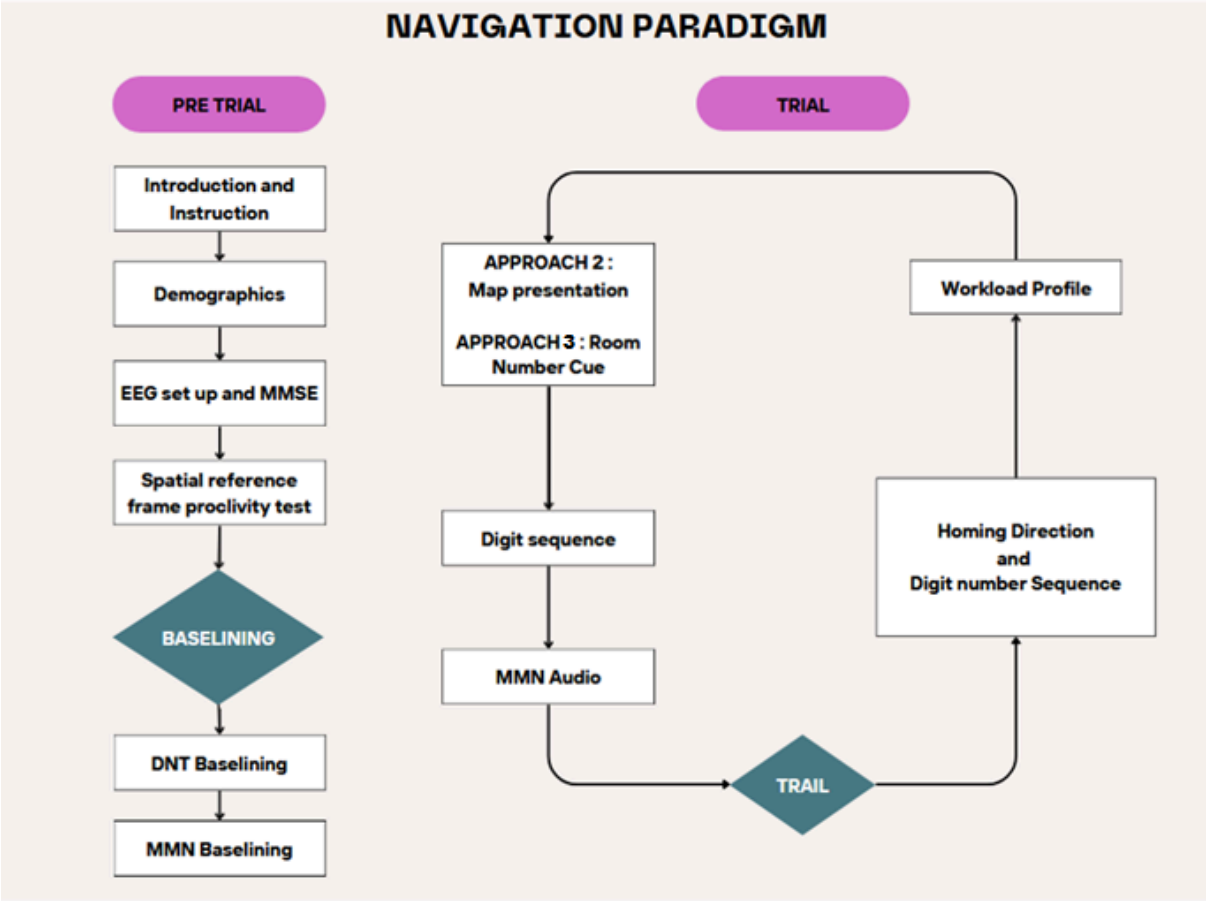

Fig 2.10: The complete protocol of the experiment. Approach 2 and Approach 3 differ in the navigation destination information presentation

The complete protocol is as described in the Flowchart. fig 2.8. Using Approach 2, 5 elderly persons of age >60 yrs , gender orientation : all males, were tested, evaluated and data analysis was done. 1 participant data was disregarded due to incomplete experimentation.

Elderly participants obtained a Hindi Mental State Examination (HMSE) score of ≤ 23, as devised by Ganguli using data from the Indo-US Cross-National Dementia Epidemiology Study on Dementia, indicating a stage of mild cognitive impairment.

The protocol is of two segments, the Pre-Trial and Trial.

The pre-trial consists of Introduction, set up , and baselining segments. Introduction to the experiment , equipment and instructors, MMSE and Demographics questionnaire is followed by EEG Set up using MBT Smarting Pro Cap, 32-channel, recorded over MBT Streamer , *Standard32* settings, sampling frequency of 500 hertz

and 250 hertz along with Accelerometer, Gyroscope and 3D orientation information, recorded over device and System.

Participant specific psychometric curve is analysed with tasks ranging from length 1 to 9 with 7 seconds of time interval between stimuli and recital. This is orally administered. From the curve , a low, medium and high threshold is characterized for each participant.

The auditory oddball paradigm is implemented using the matlab interface, Using BeepSound plugin. All of them integrated over LSL (designed by 2020 Swartz Center for Computational Neuroscience), and through LabRecorder App (Copyright (c) 2012 Christian Kothe).

Spatial Reference proclivity test : This task demonstrates how to check the RFP of the participant based on their reaction on video screening. The Egocentric and Allocentric orientation of the participant is calculated by presenting a monotonous tunnel with right or left orientation turn in a total time of 12 seconds. This conclusion stems from the observation that participants displayed a preference for either an egocentric or allocentric reference frame when solving the task (Gramann *et al.*, 2005).

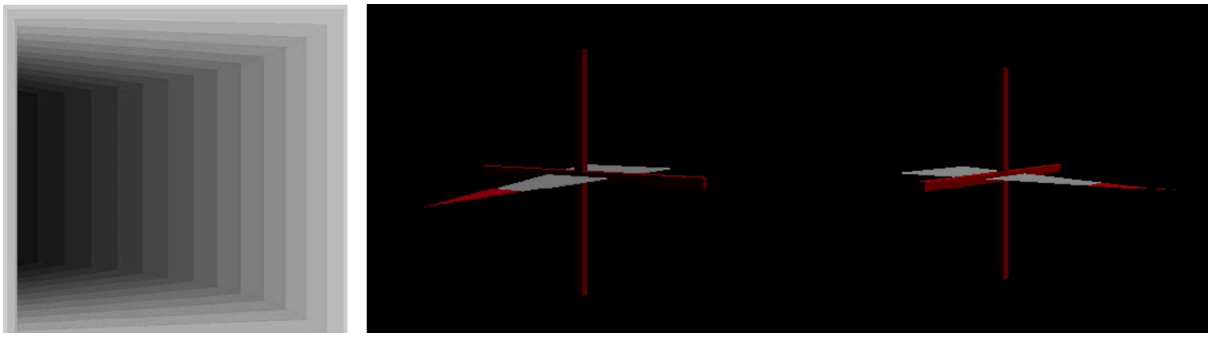

Fig 2.11: Spatial Reference Proclivity test. Left : depiction of the tunnel involved in turns. Right : Tunnel turn orientation is evaluated using this prompt to gain information on the participants Allocentricity and egocentricity. Left and Right turns are depicted at random for a total of 20 trials and their Ego, Allo measure is calculated.

The Trial consists of 4 sessions of navigation. The four trails are formulated with characteristics of Navigation : Working memory load to be the following. The navigation displacement is between Homing Direction and Target Position, Homing

angle is the direction angle from Target Position towards Home Direction. Working Memory difficulty is based on the baselining.

SESSION 1 : Longer displacement, Obtuse Angle, Difficult DNT

SESSION 2 : Shorter displacement, Acute Angle, Easy DNT

SESSION 3 : Shorter displacement, Acute Angle, Difficult DNT

SESSION 4 : Longer displacement, Obtuse Angle, Easy DNT

The paradigm was performed at 4th Floor, Engineering Building 2, IIT Kanpur, Kanpur, India, with a setting of 35 rooms.

APPROACH 3

MODIFICATION 1: Successful completion of the test trials does not require any training component within the task itself and reduces prior participant exposure to the layout of the supermarket by offering only a brief practice trial. At the commencement of testing, participants are offered a practice trial involving a 5-meter walk with one turn, serving to acquaint them with the indoor environment and ensure comprehension of task instructions. The addition of the practice trail is to ensure that participants understand that the question focuses on the direction taken from the starting point to the ending point, rather than the exact path followed. Additionally, the practice trial serves to familiarize participants with the sequence of the paradigm and the nature of the questions posed.

SESSION 1 (Test Session) : Constitutes a 10 m travel with one right turn, with DNT difficult be HIGH.

Subsequent sessions remain as defined.

MODIFICATION 2 : In lieu of employing map-based presentations, participants are instead furnished with room numbers as cues, which are distributed as cue cards at the commencement of the protocol. Rooms within the experimental setting are designated with numerical identifiers ranging from 111 to 555, each corresponding to one of five target destinations. Additionally, five irrelevant rooms are assigned random numbers within the range of 510 to 524. While the sequence of target

locations aligns with that of approach 2, this modification is aimed at reducing reliance on initial visual representations and memory of the provided map, thereby fostering a sense of disorientation among participants and enhancing immersion within the experimental

Using Approach 3, 3 Participant data was collected, 1 of a healthy 32 year old participant (FPDemo) and 2 older (60 years above) participants of both genders(FP01, FP02) was collected. Male participant data (FP01) was disregarded due to lack of auditory perception.

Chapter 3 **Results and Discussion**

3.1 BEHAVIORAL MEASURE ANALYSIS

The below image, (Fig 3.01) is a visual representation of the variation of pattern of responses between different participants and between Approaches.

Accuracy angle error is calculated by the magnitude of difference between the Homing Angle response provided by the participant and the accurate Homing Angle.

Approach 1 Sessions 1-4 is equivalent to Approach 2 Sessions 2-5.

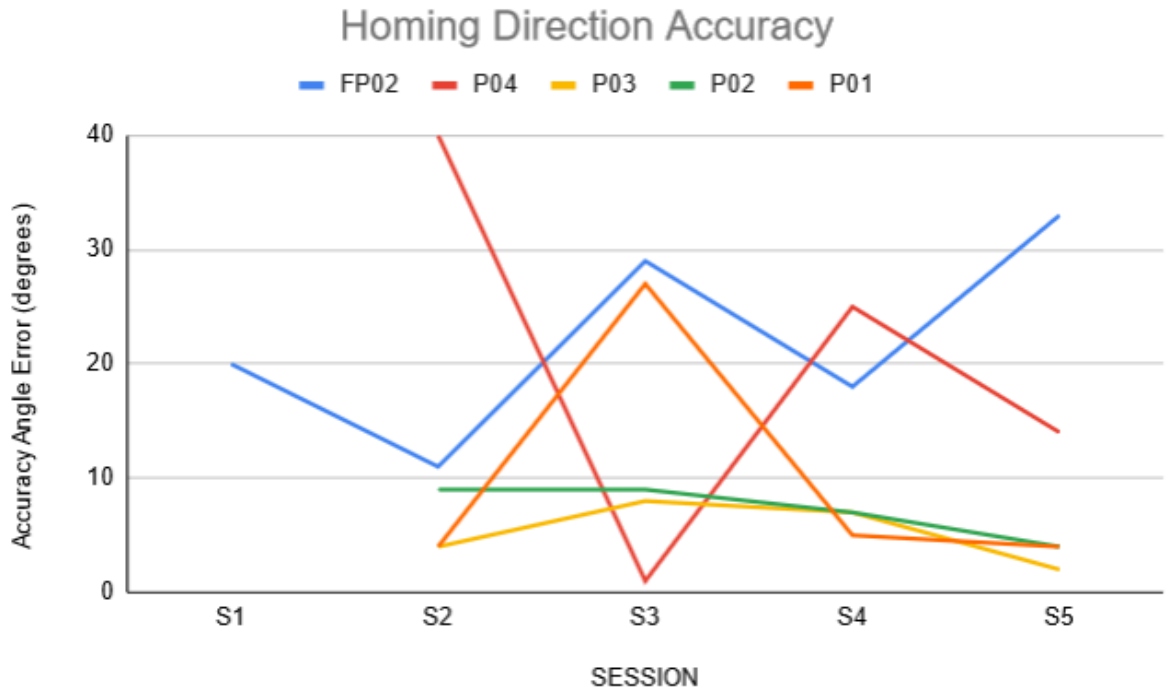

Fig 3.01. Homing Direction Accuracy. It is measured by the difference between the participant's response to homing angle question and accurate Homing Angle from the Target Position.

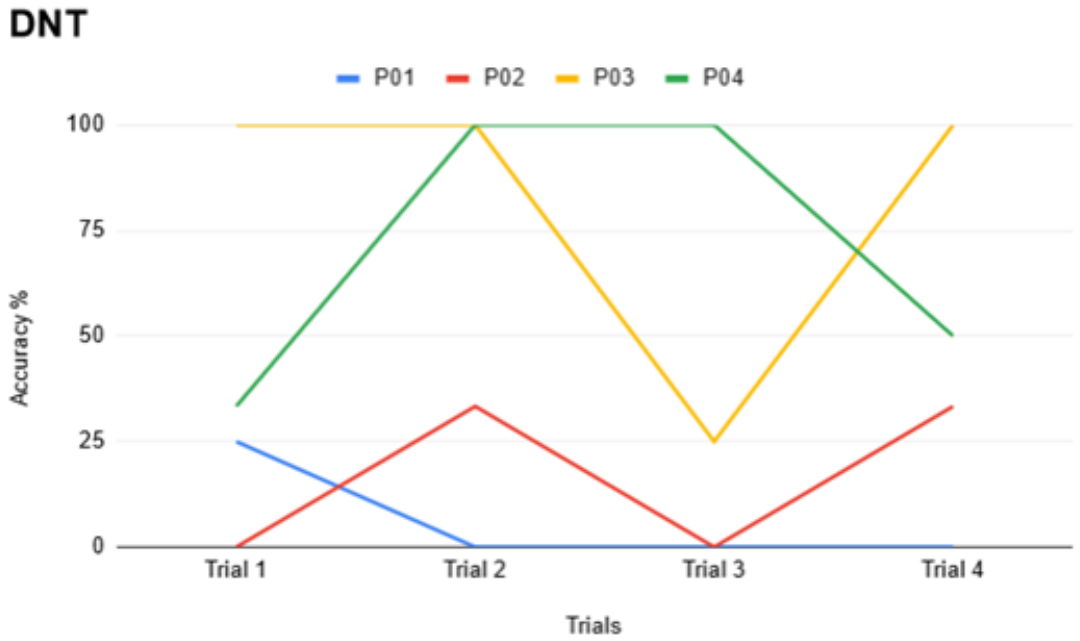

Fig 3.02 : Visual Plot of Accuracy percentage of the Digit Numbering Task

Fig 3.02 provides the Accuracy percentage of the Digit Numbering Task. Here the percentage accuracy is calculated by the percentage of numbers accurately recited back by the participant at the end of each trail. There is however no standard deviation representation and the data is highly skewed towards 100 percent or 0 percent, and present no pattern between participants nor sessions.

Figure 3.03(a) Represents travel time for each navigation session for all participants(including Approach 1 and Approach 2)

In Figure 3.03(b) for Normalised travel time, Session 1 is shown to consistently have the highest travel time. However this could be attributed to novelty of the paradigm and it can explain the reduced time for session 1 in FP02.
Travel time and Digit Numbering Accuracy do not seem to represent a pattern ‘within’ themselves across sessions which doesn't yield to a significant relation ‘between’ them. Enhancing participant data and instructor-devoid navigation can help provide us insight on these measures and their significant relation or lack of relation.

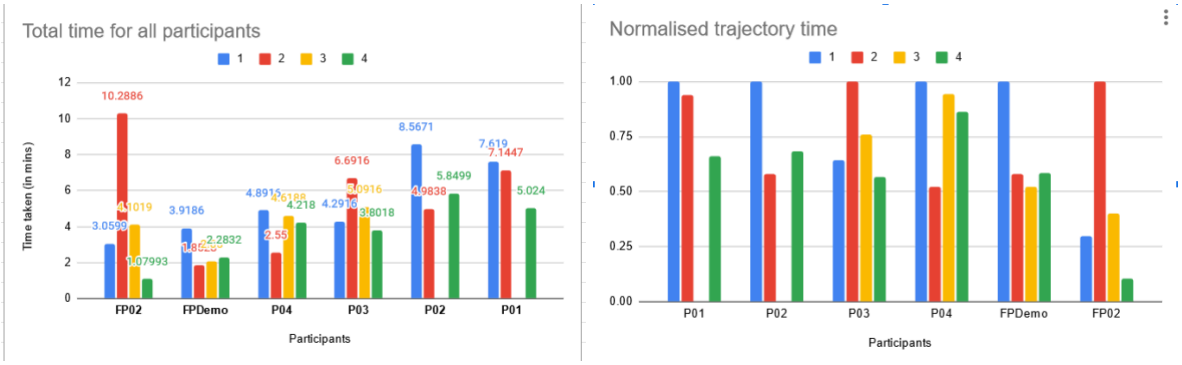

Fig 3.03 {a,b} : Navigation Travel Time analysis

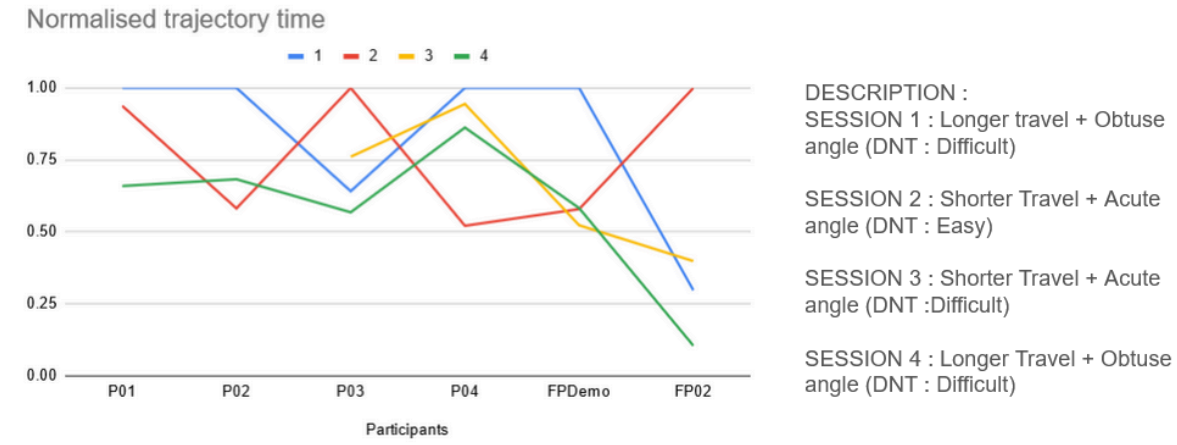

Fig 3.04 : Visual Representation of Normalised travel time for each participant with description

Participant	Allo	Ego
P01	0.25	0.75
P02	0.4	0.6
P03	0.55	0.45
P04	0.5	0.5

```
userResponseNonZeros = userResponse(all(userResponse,2),:);
egoType = sum((userResponseNonZeros(:,2)==1))/length(userResponseNonZeros);
alloType = sum((userResponseNonZeros(:,2)==2))/length(userResponseNonZeros);

if egoType > 0.7
    rfpType = 'EGO';
end

if alloType > 0.7
    rfpType = 'ALLO';
end
```

Fig 3.05(a,b) : Egocentric and Allocentric Task results along with numerical calculation representation for allo and ego measures.

Fig 3.05 shows the result of Egocentric and Allocentric tasks. A participant's orientation is termed as Egocentric or Allocentric if Ego or Allotype (in Fig 3.5) respectively is above 0.7. This enables us to further categorise spatial navigation patterns, if any.

3.2 TRAJECTORY ANALYSIS

In this paradigm, we cannot use GPS or satellite location estimation as the navigation set up is inside a building. Even though Mobile GPS accuracy is measured to lie between 7 - 20 mts (Merry and Bettinger, 2019), since our paradigm is indoors, the accuracy drops dramatically such that the horizontal GPS accuracy error is almost 300 mts (Zandbergen and Barbeau, 2011). Hence we cannot incorporate GPS to Map Trajectory Path.

Hence we used IMU (Inertial Measurement Unit) based path estimation. In approach 1, we use an in-built inertial sensor in the EEG cap device. The inertial parameters used are accelerometer, gyroscope, and Magnetometer.

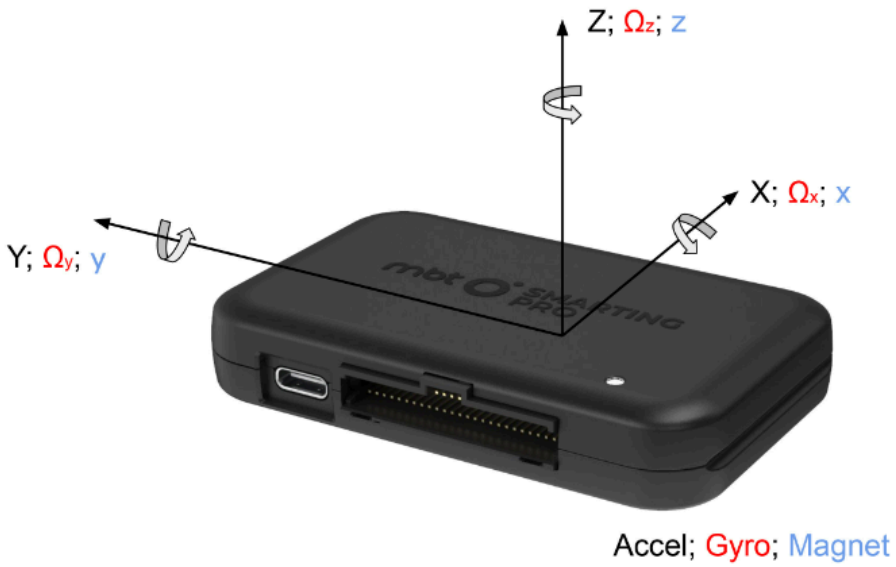

Fig 3.06 : The MBT Smarting Pro Device orientation. It has inbuilt IMU sensors (Accelerometer and Gyroscope) situated in the orientation provided below. It is placed in a upright orientation (+ X axis perpendicular to the ground) where subject's rotation is measured by rotation around X axis and forward motion is obtained from translation in z axis

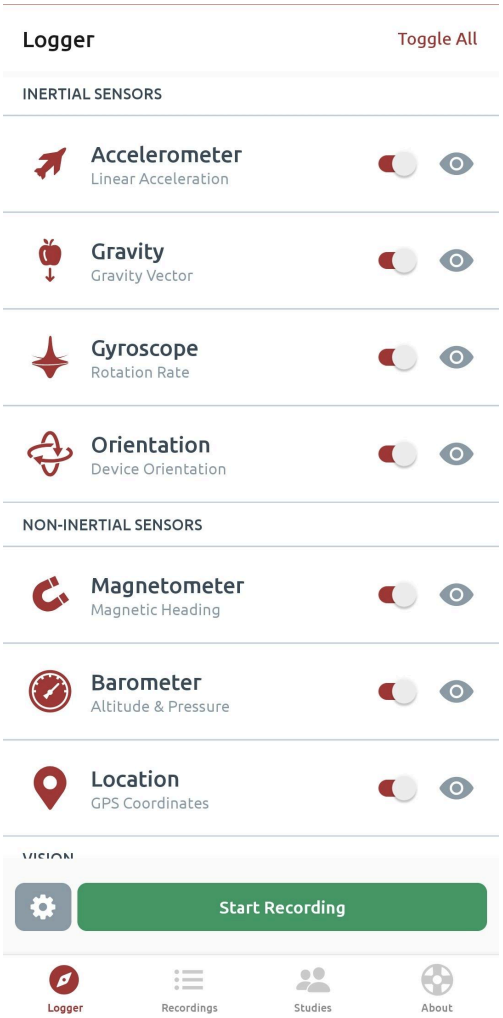

Fig 3.07: Sensor logger interface. This paradigm uses inertial sensors such as Accelerometer and Gyroscope measurements.

We translate these readings obtained along with EEG data at a frequency of 250 hertz, or 500 hertz. It is downsampled to a walking speed frequency of 0.5 hertz and plotted (after standardisation to walking speed). Here, We integrate two axis data from two inertial parameters (accelerometer and gyroscope) to obtain the path travelled by the subject. Position and orientation vectors are derived from a translational , forward and backward movement accelerometer axis (A_x) and a lateral rotational gyroscope axis (G_y), by integration of these measured vectors. Script source used along with description is provided at this link reference.

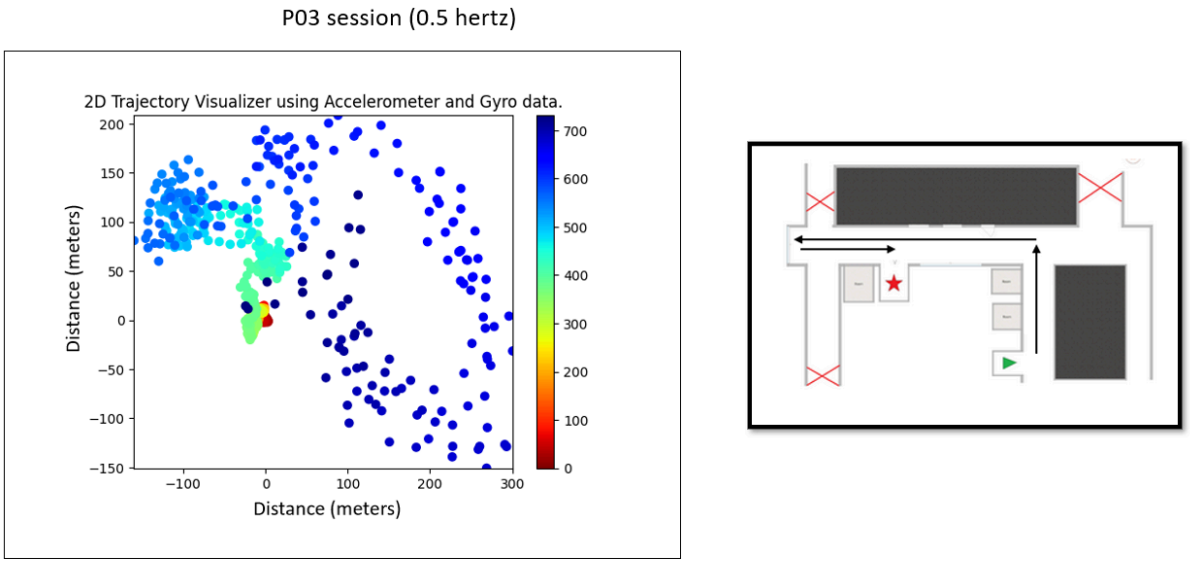

Fig 3.08: This is an example trajectory plot obtained from Approach 1 from participant P03. (a) A visual representation of the path observed. (b) The trajectory path plot from translation from an IMU sensor.
The heat map represents the data points with respect to time progress. (Red to Blue represents initial to end travel data points) The total time points is also represented in the heat map bar on the right of each path plot.

The sensitivity ranges of each parameter is as described in Fig ()

SENSORS	PARAMETERS	VALUE
Accelerometer	Range	+/- 4g
	Bandwidth	62.5Hz
	Resolution	14 bits
Gyroscope	Range	2000 °/s
	Bandwidth	32 Hz
	Resolution	16 bits
Magnetometer	XY Repetition	15
	Z Repetition	16
	Resolution	13/13/15 bits

Fig 3.09: The different sensitivity ranges observed in inertial meters of MBT Streaming Pro EEG Device.

In approach 1, the trajectory plotted failed to replicate the trajectory path accurately. An example comparison is provided in Fig x(). The device is also required to be reset to original orientation (appropriate orientation) at the start of each trail. Hence there was a requirement for change in Approach 2.

Furthermore, trajectory estimation for MBT Sensor Device was performed using the mentioned protocol to obtain trajectory for snippets of short periods of time. During integration of longer duration of data,
We observe an integration error called GyroDrift occurring due to constant changing non zero readings of a gyroscope. Change in orientation of motion is obtained from Angular velocity which is obtained from an integral function of gyroscope readings. When acceleration measurements are incorporated for path estimation, the error blows up in magnitude. As the travel time or recording time increases, accumulation of this error is observed.

Hence there was a requirement to select and calibrate an IMU sensor.
Here we used an App called Sensor Logger (developed by Kelvin Choi, from Velrann, United Kingdom) compared and standardized it against the inbuilt IMU sensor of MBT Smarting Pro Device.

The standardization procedure consists of 5 tests between MBT Smarting Pro Device and Sensor logger app, developed by Kelvin Choi, from Velrann, United Kingdom. Each of these tests involved testing the detection of change in orientation (by 180 degrees) around a specific axis. We expected to see clear deflection and representation in the axis of change and consistent constant in other axises.
TEST 1 to TEST 4 were of 20 seconds with the change in orientation induced at the 10th second. TEST 5, To and Fro was a motion test with a single to and fro motion starting at 10 seconds of recording and spanning 3 m to and fro in a motion of uniform velocity (time duration : 25 seconds) and a 180 degree rotation at around 26th second for a span of 18 seconds.

TEST	Description	EXPECTED VARIATION A_i = a ms^2 G_i = g °/s
Stationary	Stationary	A_i = 0, i = z, y , A_x = 9.8 G_i = 0 for all i,j = x,y,z
Roll 180	180° Rotation of sensor around X axis	G_x fluctuation
Pitch 180	180° Rotation of sensor around Y axis	G_y fluctuation
Yaw 180	180° Rotation of sensor around Z axis	G_z fluctuation
To and Fro	3m walking span + 180° Roll + 3m walking span	A_z and G_x fluctuation

Table 3.10 : Test Description for IMU sensor calibration Default measurements expected. Ai = 0, i = z, y , Ax = 9.8 , G_i = 0 for all i,j = x,y,z}

The fig 3.10 below, device data represented high amounts of noise in accelerometer and gyroscope readings in axis that were not perturbed to change. The sensor might to be too sensitive to variations and could lead to accumulated error during integration for path estimation.

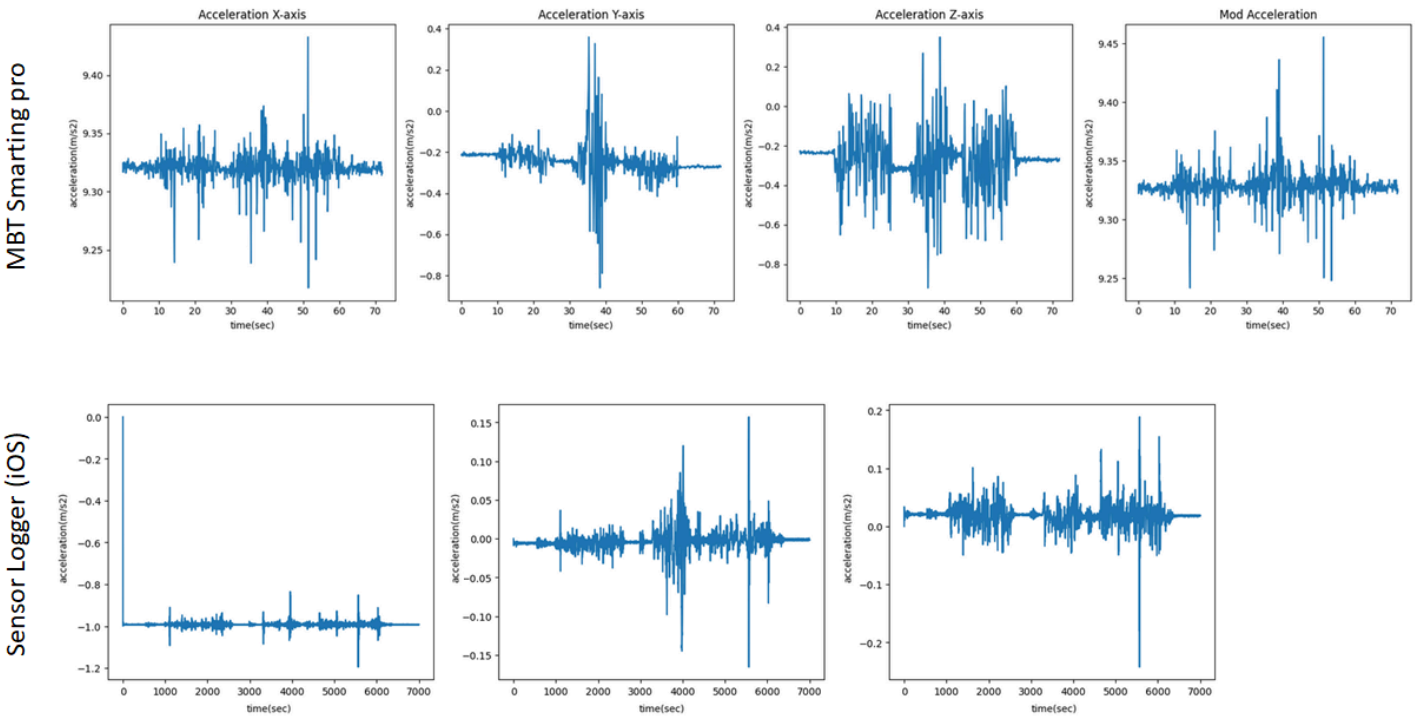

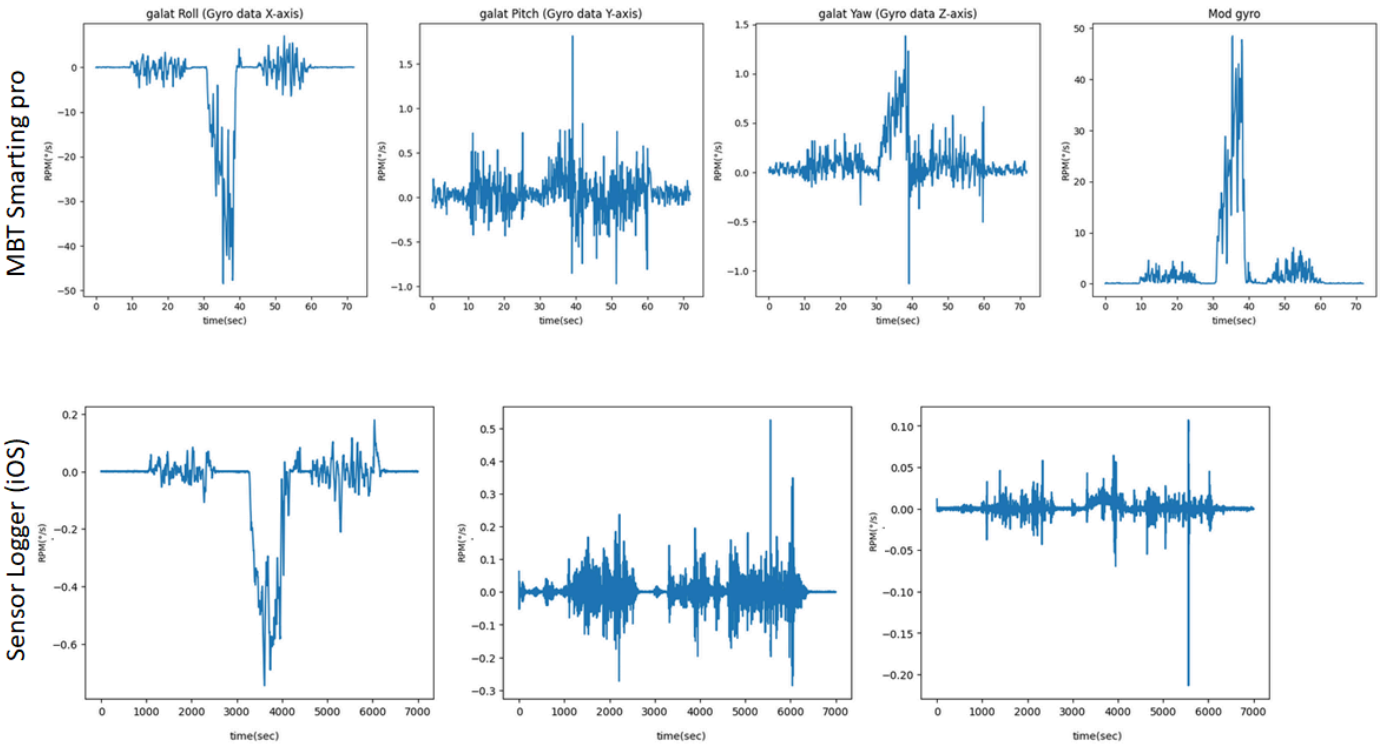

Fig 3.10: the Accelerometer and Gyroscope profiles for TEST 2, Roll 180, as a comparison between Device and Sensor logger. Acceleration in X direction in sensor logger is gravity corrected (normalised for acceleration due to gravitation in the negative direction).

We can observe a high amount of fluctuations leading to integration error accumulation and gyrodrift.

Therefore the device has more noise, hence sensor logger data was analysed.

GYRODRIFT CORRECTION

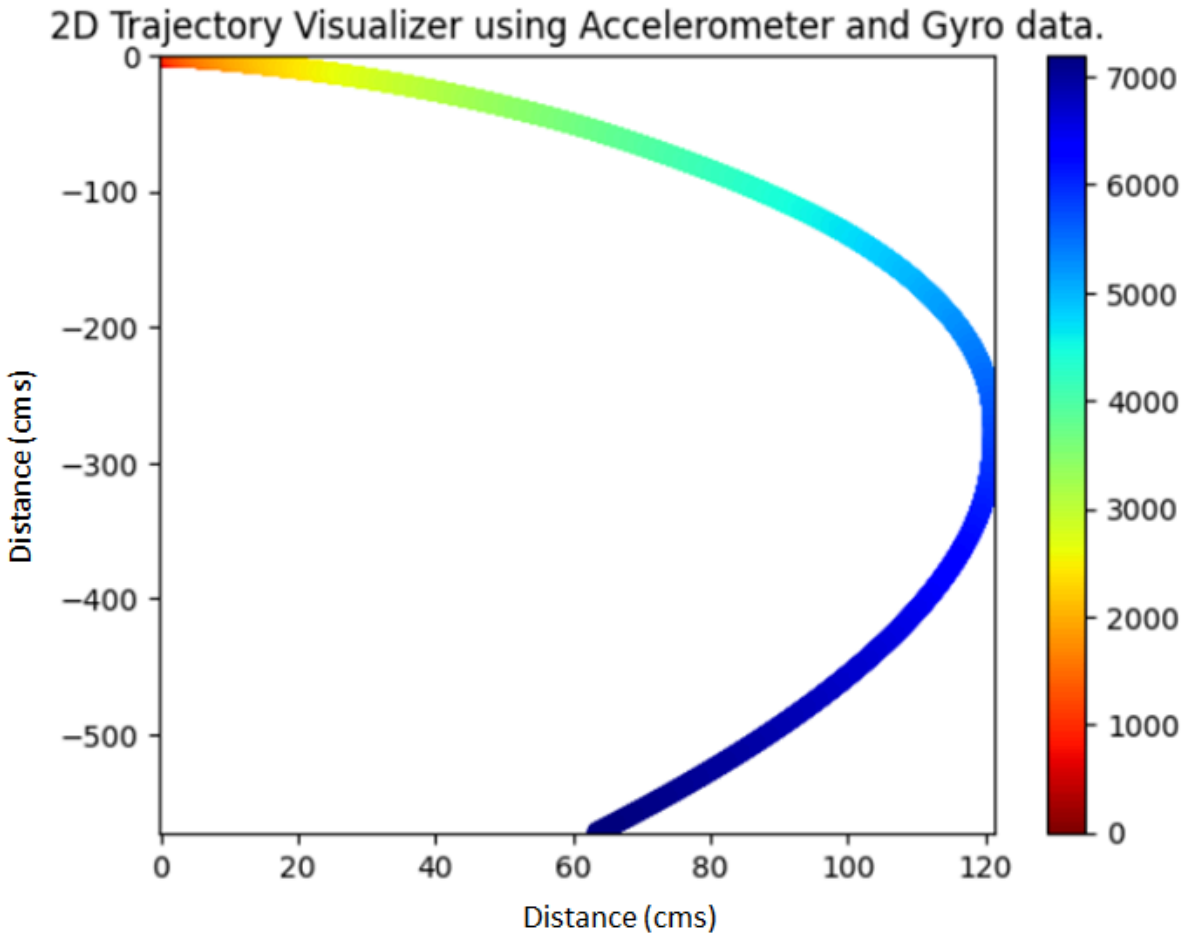

Fig 3.11: Representation of a gyrodrift for a straight line motion and back for 3 m. It can be observed that there is a drift of almost twice the distance (6 m). This also leads to an approximate 0.6 m lateral drift from the mean position. This test too was initiated at 10 seconds of the start of recording, and this initiated the drift irrespective of the stationary position. Sampling rate was of 10 hertz and movement of approximately 60 seconds.)

To correct integration bias arising from non zero data ,an analysis standardisation procedure was explored.

TEST 0 (RECTANGULAR) A rectangular path of 3 m * 1 m was travelled with constant velocity and used as a test to calibrate the path estimation python script. The over-estimation and integration bias was also tried to be corrected with Kalman filter (with its unit matrices modified to accommodate the sensor sensitivity). The over-estimation occurs because of the accumulation of integration errors from accelerometer and gyroscope readings which causes the position estimation to be erroneous.

Corrections :

1. The magnitude of acceleration and gyroscope values are incorporated to reduce negative deflection of integrated data. The numerical characteristics (positive and negative variations) steer the orientation integration to either side of the mean values of acceleration and gyroscope.
2. Data of the first 5 seconds is eliminated. The Test initiates from 10 seconds after the onset of recording. The mobile device is stationary till the 10th second. This is to ensure that there is no accumulated error resulting from fluctuating gyroscope values.
3. Accelerometer data is filtered with a threshold of 1.1m s sq , any variation values below 1.1 m sq was referenced to 0. This is to ensure that any insignificant movements usually resulting in accelerometer deflections of minute deflections (lesser than 1 m s sq) are filtered.

Hence the correction mechanisms that are incorporated for further are providing a threshold on accelerometer reading incorporated for path estimation analysis. This enables lesser error propagation when it is integrated with gyroscope translation into orientation estimation. Correction 2 is very essential as it is significantly important to feed the right segment for integration without polluting with initial and certain noise.

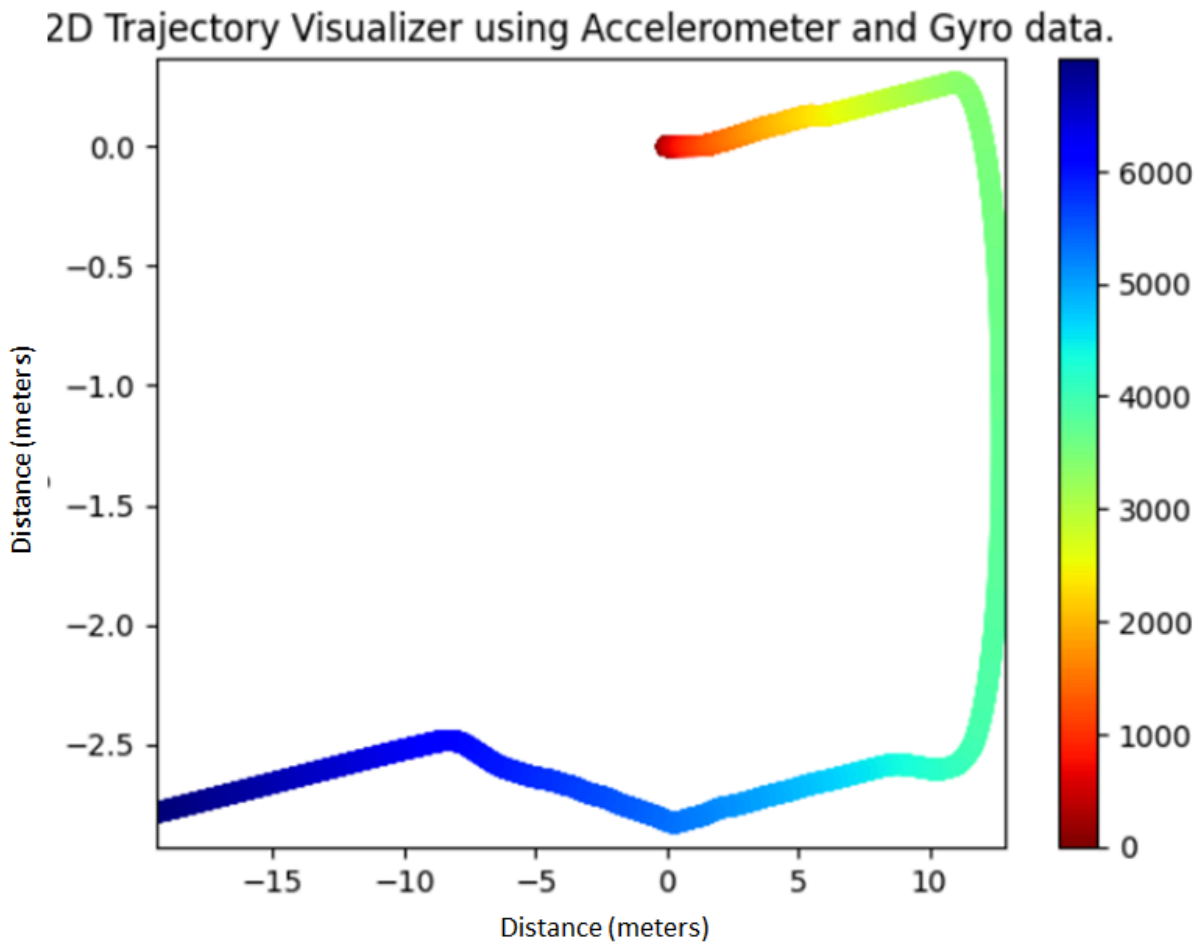

Fig 3.12: Normal path estimation plot using TEST 0 RECTANGULAR measurements. Frequency of 200 hertz, with 35 seconds of data.

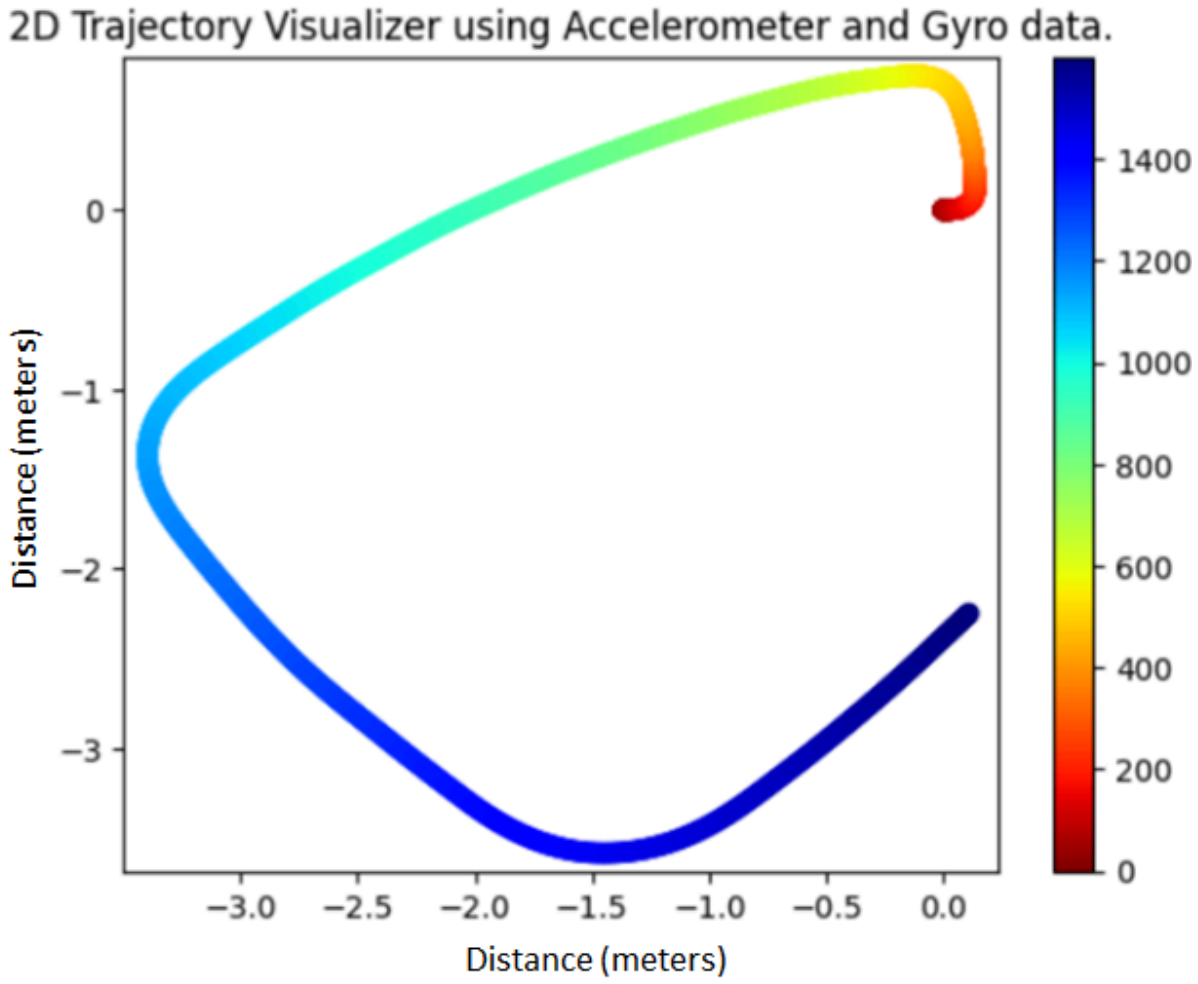

Fig 3.13: Path estimation plot . Correction terms 1,2 and 3 are applied. Data selected between 5 seconds of onset and end (30 seconds) of downsampled frequency of 50 hertz. Acceleration values are thresholded at 1.1 m s sq.

3.3 ERP ANALYSIS

Offline processing and analysis of EEG data were conducted by using scripts, which incorporated functions present in the EEGLAB Toolbox25 for MATLAB R2021a (the MathWorks, Natick, MA, USA). The data was initially subjected to a high-pass filter with a bandpass set between 0.5 and 40 Hz. Continuous EEG data were then subjected to a channel rejection algorithm that searches for problematic channels based on values of covariance and standard deviation with neighboring channels(Iterative Standard Deviation method). Channels that were rejected underwent a spherical interpolation method present in EEGLab. Afterwards, the data were segmented into epochs beginning 250 ms before each tone was presented and lasting post 1 s after stimulus onset. Here the epochs were of two characteristic types based on the oddball paradigm (Standard and Deviant). The identification of

bad channels follows the labeling described in (Komosar, Fiedler and Haueisen, 2022) and Independent Component Analysis is performed using the function RUNICA in EEG . Bad channels are rejected and don't have more than 10 percent brain component and as criteria described in (Komosar, Fiedler and Haueisen, 2022). Following this, baseline correction was done to the 500 ms pre-stimulus interval for each epoch, of both standard and deviant. Epochs deemed poor were automatically rejected using autorej with a threshold of 1000 microvolt channel response. The probability threshold in standard deviation of epoch data for detection was set at 5.

Next, the epochs were averaged based on the stimulus condition to produce the auditory evoked potential for both the standard and deviant tones.

3.3.1 ERP Profiles for Each Block, for Each Participant

Fig 3.14 - 3.24: show the Event Related Profiles Plots for each participant in each session. Session: Baseline Open and BaselineClosed represent Baselining MMN tasks administered during the initial 4 minutes with participation resting with eyes open and eyes closed , respectively. The 4 participants from the Approach 1 Paradigm are P01, P02, P03, and P04, and the session tags are S01, S02, S03, S04. The Standard curve in each plot represents EEG data for all standard epochs averaged over 32 channels after preprocessing defined above, and the Deviant data is derived from epochs representing deviant stimuli.

The auditory stimuli onset in the following graphs is at 500 ms.

The Participant ID for Approach 2 Paradigm are tagged as FPDemo, FP01 and FP02.

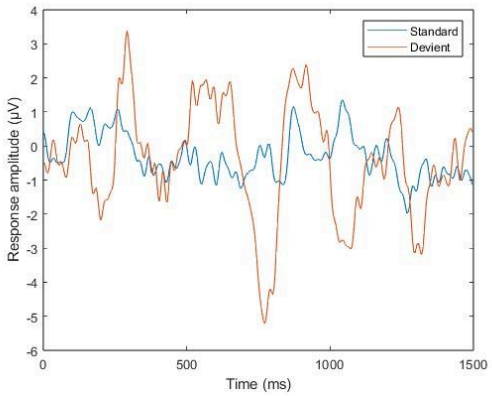

Fig 3.14: P03S01

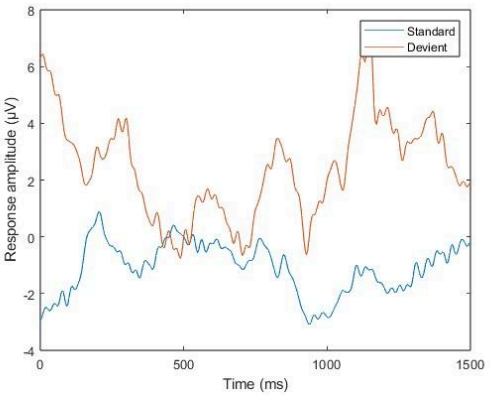

Fig 3.15: P03S02

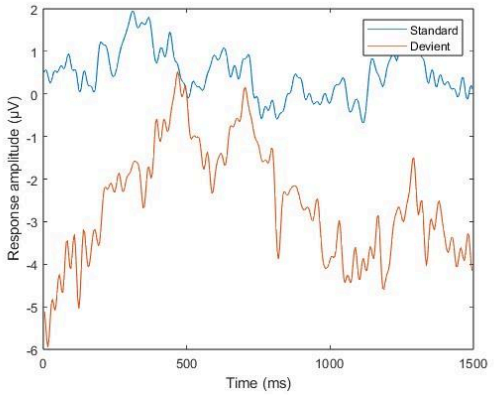

Fig 3.16: P03S04

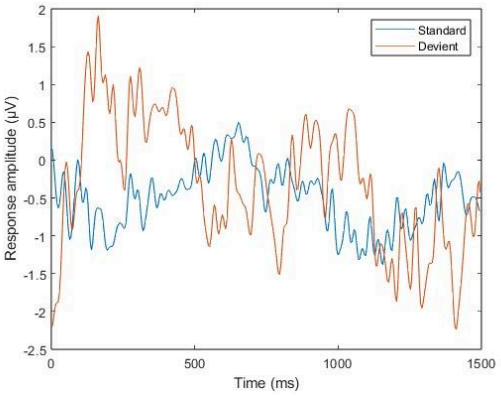

Fig 3.17: P03BaselineOpen

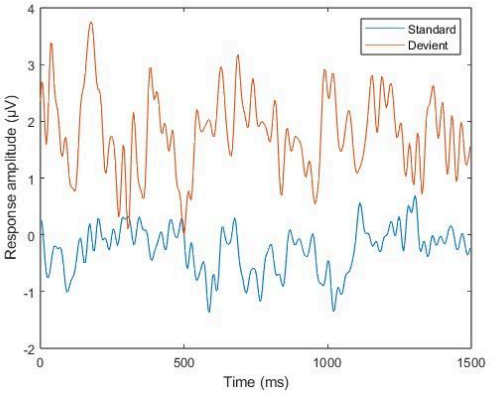

Fig 3.18: P03BaselineClosed

Fig 3.14- Fig 3.18 : P03 Event Related Potential for 4 blocks

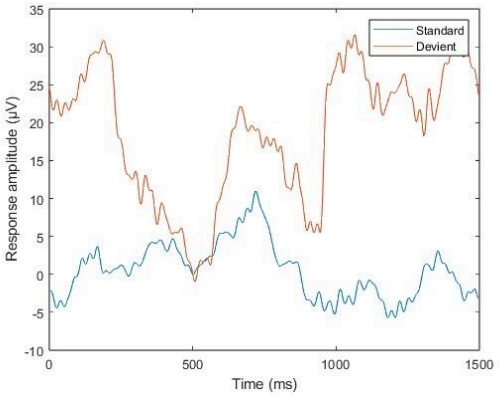

Fig 3.19: FP02S01

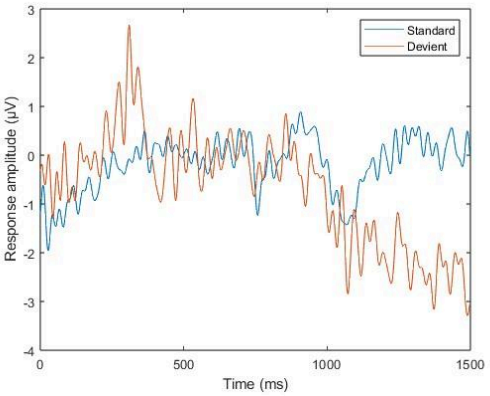

Fig 3.20: FP02BaselineOpen

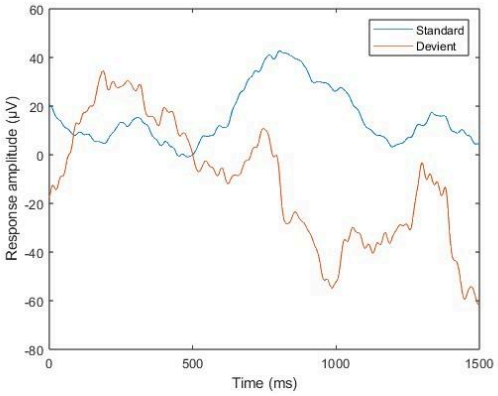

Fig 3.21: FP02S02

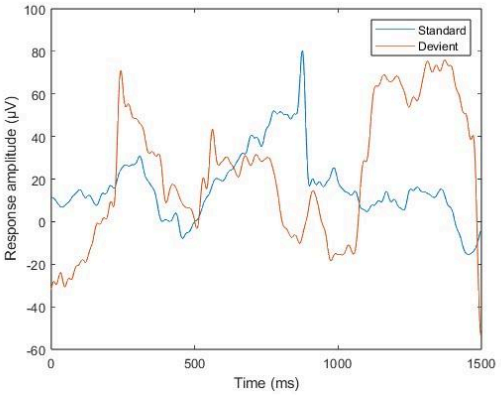

Fig 3.22: FP02S03

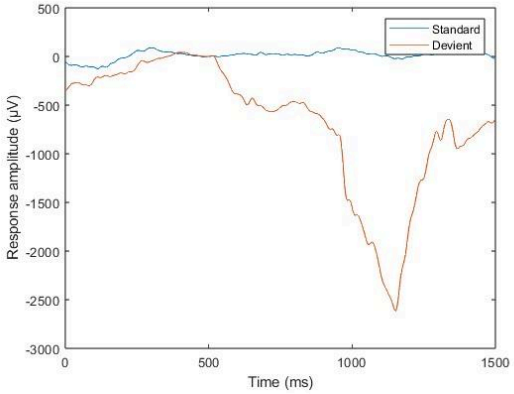

Fig 3.23: FP02S04

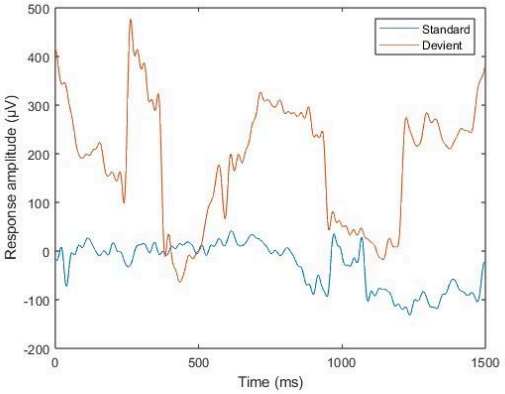

Fig 3.24: FP02S05

Fig 3.19- Fig 3.24 : FPDemo and FP02 Event Related Potential for 4 blocks

3.3.2 ERP Profiles for averaged across blocks, for A Participant

Fig 3.25- 3.26 shows single channel data for all the 32 channels. EEG data for each Standard and Deviant Epochs across all sessions are concatenated and averaged for each single channel

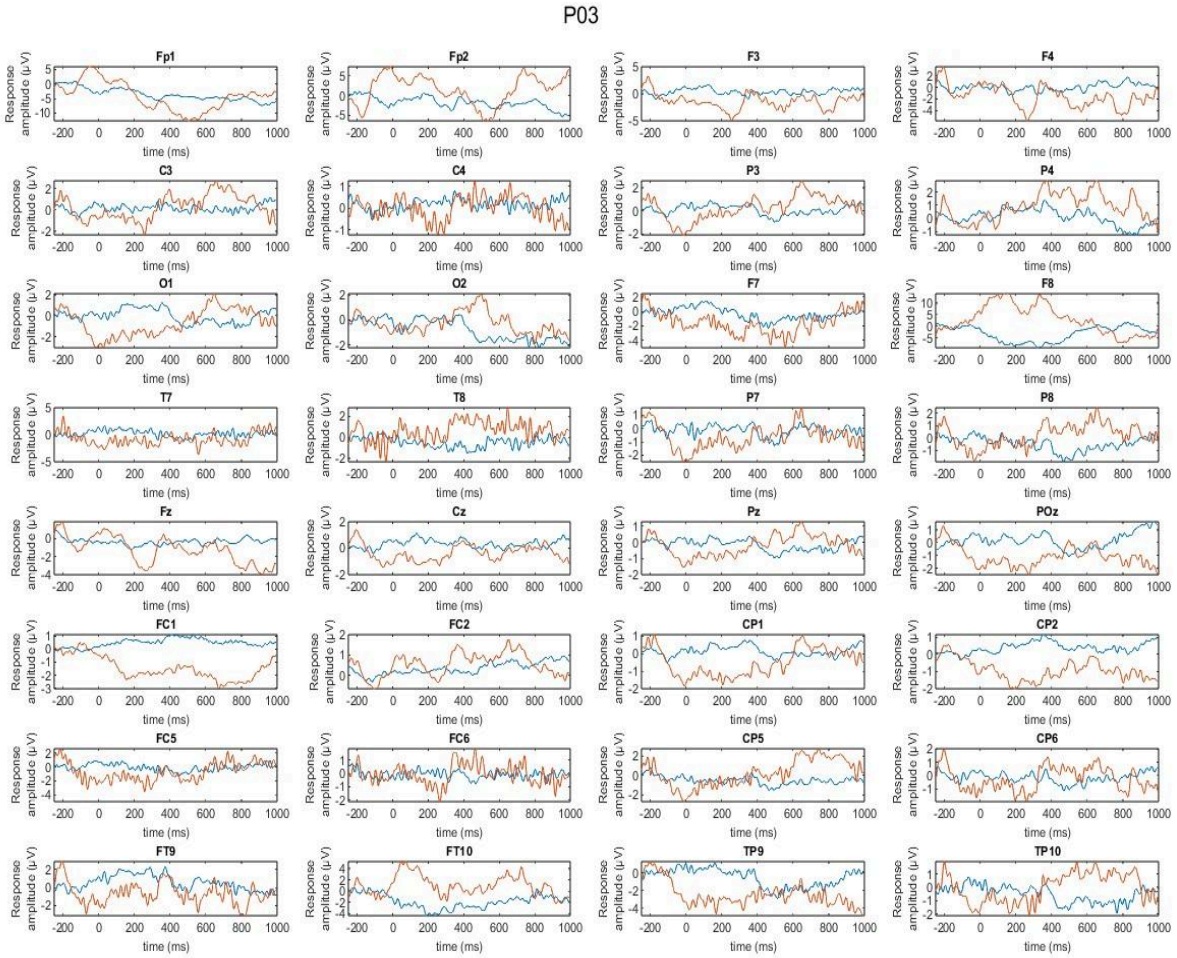

Fig 3.25: P03 single channel ERP Profiles for all the 32 channels

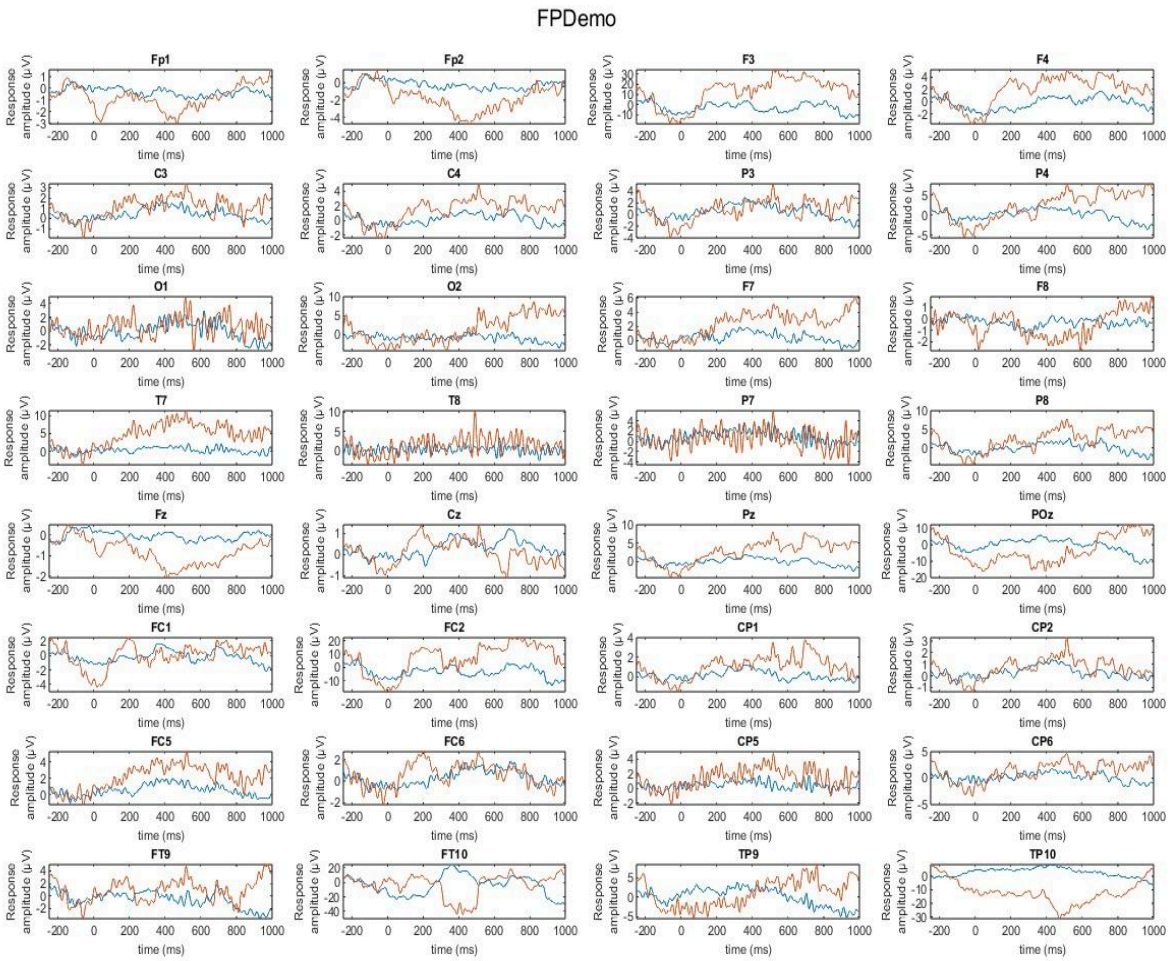

Fig 3.26: FPDemo single channel ERP Profiles for all the 32 channels

3.3.3 ERP Profiles for averaged across blocks, averaged across channels for Each Participant

Fig 3.27 - 3.33 represents ERP Profiles averaged across all respective good channels with EEG data concatenated across all sessions. The stimuli onset at 0 mark on the X Axis.

To significantly categorize the difference, Standard deviation error bars with respect to the epochs are plotted using Recampbell: ShadedErrorBar function using Matlab 2022.a version.

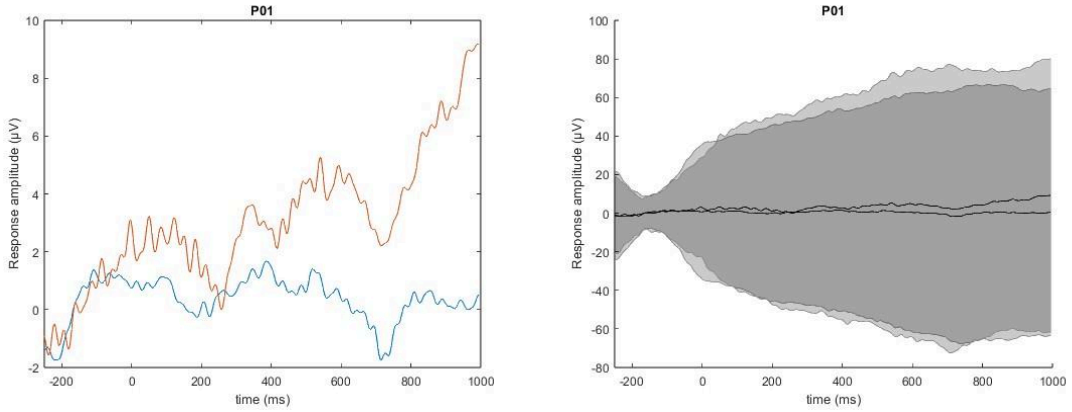

Fig 3.27{a,b} : Left ,P01 channel and session averaged ERP plot. Right, Standard error bar over fig 3.34a.

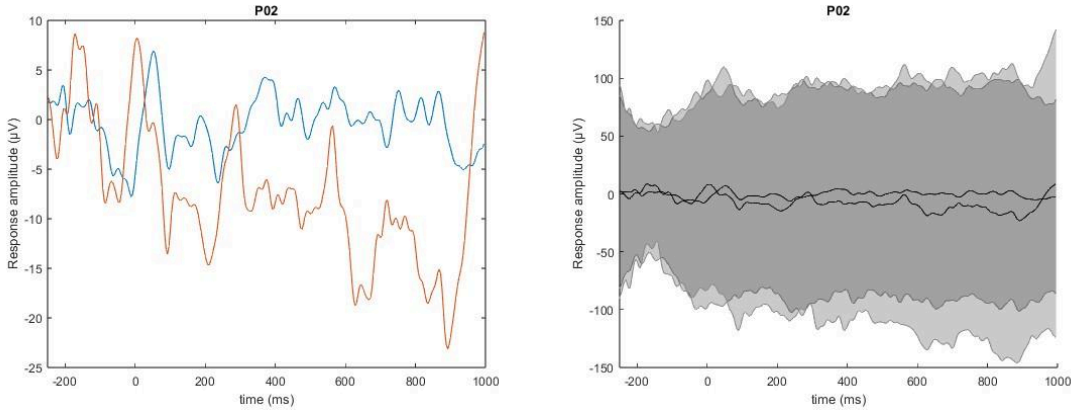

Fig 3.28{a,b} : Left ,P02 channel and session averaged ERP plot. Right, Standard error bar over Fig 3.35a.

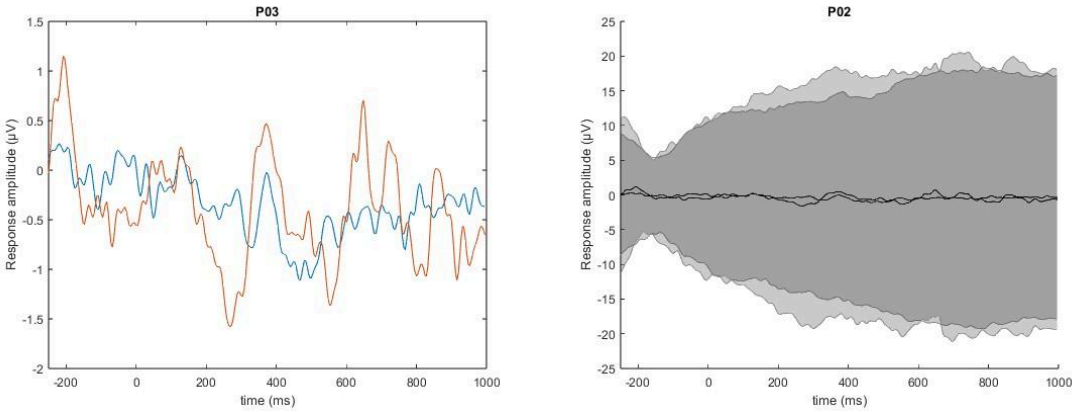

Fig 3.29{a,b} : Left ,P03 channel and session averaged ERP plot. Right, Standard error bar over fig 3.36a.

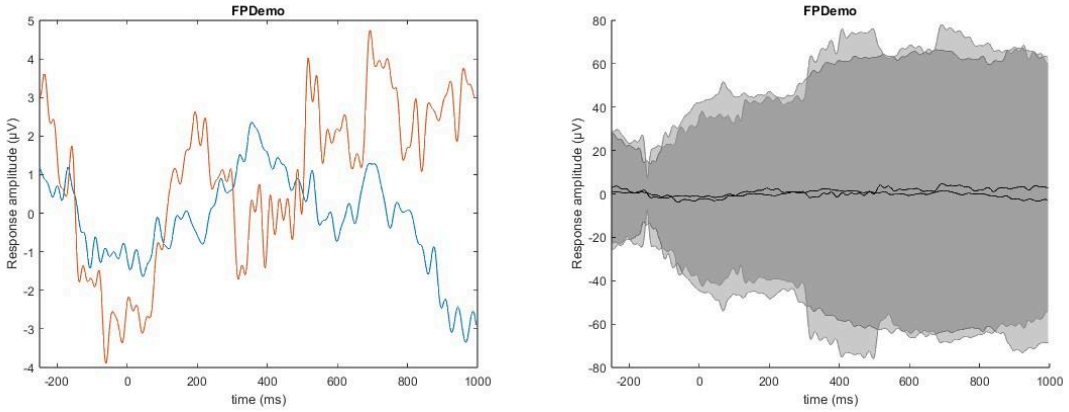

Fig 3.30{a,b}: Left ,FPDemo channel and session averaged ERP plot. Right, Standard error bar over Fig 3.37a.

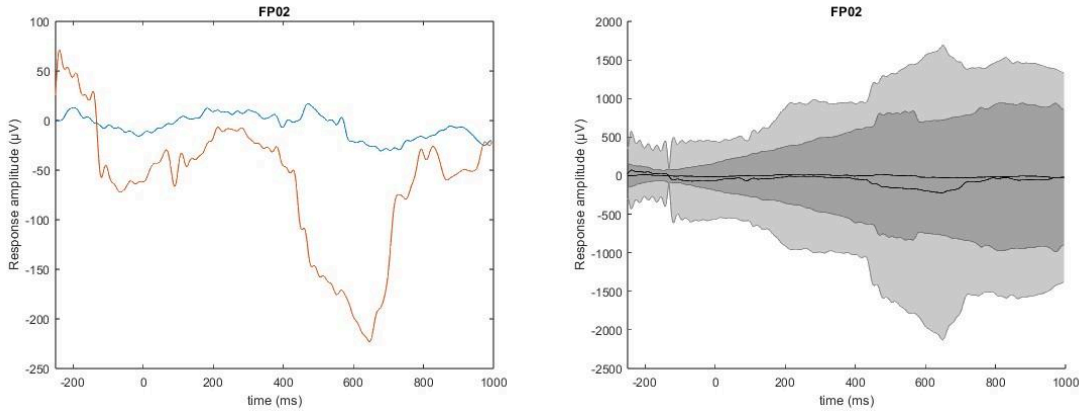

Fig 3.31{a,b}: Left ,FP02 channel and session averaged ERP plot. Right, Standard error bar over Fig 3.38a.

3.3.1 ERP Profiles for averaged across blocks, averaged across region specific channels

In order to explore changes in our regions of interest, Parietal, Central and Frontal, averaged statistics is performed on Region specific electrode data.

Below From Fig 3.39 - Fig 3.40 is an example plot for an Approach 1 Participant, and an Approach 2 Participant.

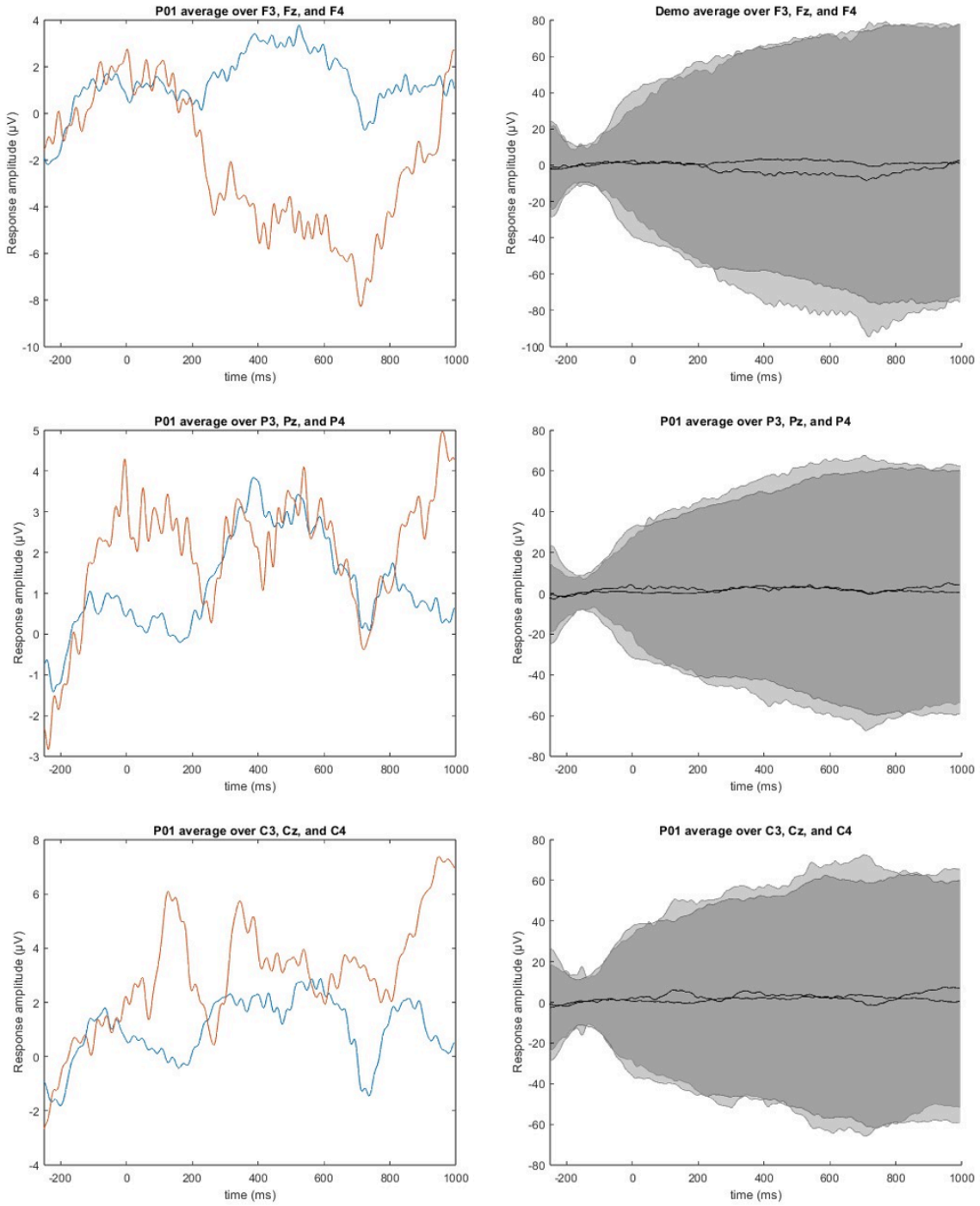

Fig 3.32: P01 Region Specific ERP plots. Parietal region ERP analysis constitutes data concatenated from P3, P4, and Pz electrodes from all sessions and averaged between them. Central brain region refers to C3, C4 and Cz electrodes and Frontal region refers to F3, F4 and Fz electrode data from the EEG data.

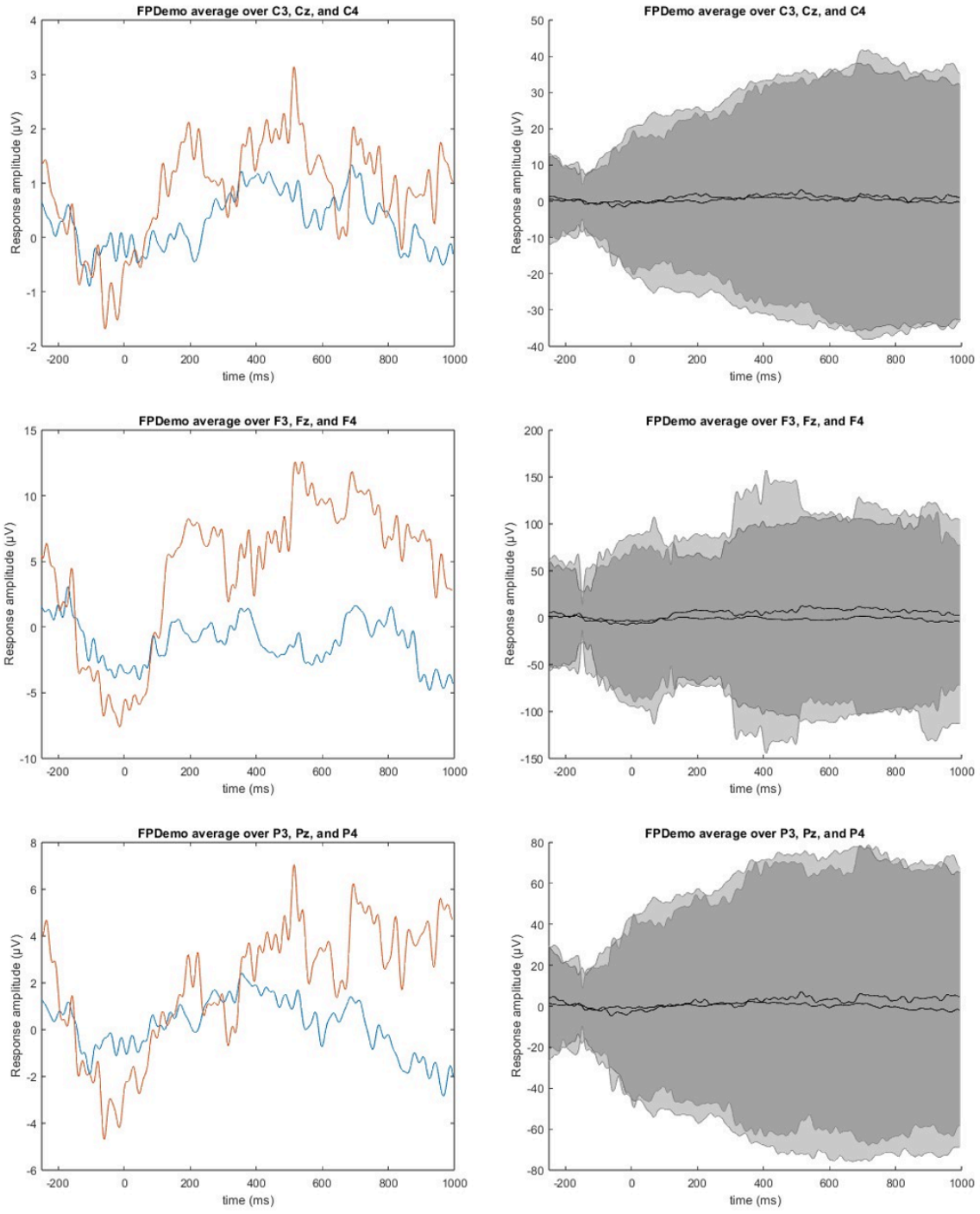

Fig 3.33: FPDemo Region Specific ERP plots

Chapter 4 Discussion

While analysing the MMN task results we aim to analyze the N1P2 and N2P3 peak from EEG data. The N1P2 and N2P3 peak is a component observed in the brain's electrical activity where The N component is an early negative deflection that typically peaks around 200 milliseconds after the deviant stimulus is presented. It is believed to reflect the brain's initial detection and processing of the deviant stimulus. Specifically, The N2P3 peak refers to the combined negative (N2) and positive (P3) deflections in the event-related potential (ERP) waveform that occur in response to these deviant stimuli.

The P3 component is a positive deflection that follows the N2 and peaks around 300 to 400 milliseconds after stimulus onset. It is associated with the brain's allocation of attention and cognitive processing resources to evaluate the significance of the deviant stimulus. Complete analysis report can be viewed after data collection.

Fig 3.14 - 3.24 : We do not observe a consistent response amplitude range nor significant baselining before the onset of stimulus.

From figure 3.25 -3.26 : We can observe the variation of pattern between different channels. We do not observe any significant difference between the standard and deviant curves for our channels of interest PZ, CZ and FZ.

Fig 3.27 - 3.31 : These averaged analysis shows better baselining and hence more reliability on the difference between Standard and Deviant.

They however do not show any significant difference between Standard and Deviant and represent high variance from epoch mean value.

In region specific analysis too we do not observe any significant differences between the stimuli responses. In this study, we found no discernible differences between standard and deviant conditions, and there was significant variation across different channel data.

Fz Cz and Pz signals are mainly used to check for the event related potentials. Cz and Pz are used to classify motor movements and spatial processing while Fz signals signify decision making and stress indication.

From these ERP Analysis plots, it proves insightful that the current EEG post processing and ERP derivation might be sensitive for a real time navigation paradigm. The behavioural set up is a complex multi modal experiment which exploits 8 domain mental resources and might be deemed important to progress

towards summary statistics of EEG data. Further Analysis is to progress with imitation with the Time Frequency Analysis of EEG data. Earlier EEG investigations incorporating both MCI and AD patients have consistently revealed neural changes compared to healthy controls. These changes encompass increased delta and theta oscillations alongside reduced alpha and beta rhythm activity, which are regarded as promising neural markers for early detection of AD due to their close links with patients' cognitive abilities. Furthermore, diminished coherence and complexity in EEG recordings, along with reduced high alpha/low alpha and ratios of theta/gamma , have also been suggested as potential biomarkers for AD diagnosis (John *et al.*, 2022)

A revised version of this paradigm that would undergo data collection of complete testing would involve all the above modifications.

Spatial navigation, containing 2 difficulties, a trial session, along with unauthorised navigation and trajectory mapping with IMU sensors planted on the subject shall yield navigation measures. Further MMN analysis would include Time Frequency Analysis, Power spectrums, Hjorth parameters providing us with 8 measures of analysis.

Our main perspective on this navigation involves viewing it as a compromised path integration. Building on the path integration example of trajectory estimation from an IMU sensor, we are attempting to investigate the causes of erroneous path estimation that occur in our brains due to stress and attention factors. Current and future research efforts are dedicated to examining effects of continuous distraction combined with memory load during navigation to investigate the interaction between working memory load and spatial navigation. This includes testing the accuracy of egocentric versus allocentric orientation as navigational measures, adjusting the navigation track to reflect real-time complexity, standardizing the difficulty of navigation paths, and ensuring that mental load levels remain the sole variable influencing the experiment. Digit numbering tasks as well as MMN are baselined.

Further data collection and analysis that is to follow shall improve statistical credibility of our hypothesis, experimentation and modelling.

Further investigations and analysis, coupled with ongoing data collection, reveal promising and potentially conclusive results that could significantly contribute to the research community.

References

1. Bjork, E.L. and Bjork, R.A. (1996) 'Continuing Influences of To-Be-Forgotten Information', *Consciousness and Cognition*, 5(1), pp. 176–196. Available at: https://doi.org/10.1006/ccog.1996.0011.
2. Braak, H. and Braak, E. (1995) 'Staging of alzheimer's disease-related neurofibrillary changes', *Neurobiology of Aging*, 16(3), pp. 271–278. Available at: https://doi.org/10.1016/0197-4580(95)00021-6.
3. Brima, T. *et al.* (2019) 'Auditory sensory memory span for duration is severely curtailed in females with Rett syndrome', *Translational Psychiatry*, 9(1), pp. 1–10. Available at: https://doi.org/10.1038/s41398-019-0463-0.
4. Cassani, R. *et al.* (2017) 'Towards automated electroencephalography-based Alzheimer's disease diagnosis using portable low-density devices', *Biomedical Signal Processing and Control*, 33, pp. 261–271. Available at: https://doi.org/10.1016/j.bspc.2016.12.009.
5. Chételat, G. *et al.* (2002) 'Mapping gray matter loss with voxel-based morphometry in mild cognitive impairment', *NeuroReport*, 13(15), p. 1939.
6. Damoiseaux, J.S. *et al.* (2012) 'Functional connectivity tracks clinical deterioration in Alzheimer's disease', *Neurobiology of Aging*, 33(4), p. 828.e19-828.e30. Available at: https://doi.org/10.1016/j.neurobiolaging.2011.06.024.
7. Drzezga, A. *et al.* (2003) 'Cerebral metabolic changes accompanying conversion of mild cognitive impairment into Alzheimer's disease: a PET follow-up study', *European Journal of Nuclear Medicine and Molecular Imaging*, 30(8), pp. 1104–1113. Available at: https://doi.org/10.1007/s00259-003-1194-1.
8. Farina, F.R. *et al.* (2020) 'A comparison of resting state EEG and structural MRI for classifying Alzheimer's disease and mild cognitive impairment', *NeuroImage*, 215, p. 116795. Available at: https://doi.org/10.1016/j.neuroimage.2020.116795.
9. Gramann, K. *et al.* (2005) 'Evidence of Separable Spatial Representations in a Virtual Navigation Task.', *Journal of Experimental Psychology: Human Perception and Performance*, 31(6), pp. 1199–1223. Available at: https://doi.org/10.1037/0096-1523.31.6.1199.
10. Hatz, F. *et al.* (2015) 'Microstate connectivity alterations in patients with early Alzheimer's disease', *Alzheimer's Research & Therapy*, 7(1), p. 78. Available at: https://doi.org/10.1186/s13195-015-0163-9.
11. Hoppe, C. *et al.* (2000) 'Digit Ordering Test: Clinical, Psychometric, and Experimental Evaluation of a Verbal Working Memory Test', *The Clinical Neuropsychologist*, 14(1), pp. 38–55. Available at: https://doi.org/10.1076/1385-4046(200002)14:1;1-8;FT038.
12. Hort, J. *et al.* (2007) 'Spatial navigation deficit in amnestic mild cognitive impairment', *Proceedings of the National Academy of Sciences*, 104(10), pp. 4042–4047. Available at: https://doi.org/10.1073/pnas.0611314104.
13. Jacobs, H.I.L. *et al.* (2011) 'Atrophy of the parietal lobe in preclinical dementia', *Brain and Cognition*, 75(2), pp. 154–163. Available at: https://doi.org/10.1016/j.bandc.2010.11.003.
14. John, A.R. *et al.* (2022) 'Unraveling the Physiological Correlates of Mental

Workload Variations in Tracking and Collision Prediction Tasks', *IEEE Transactions on Neural Systems and Rehabilitation Engineering*, 30, pp. 770–781. Available at: https://doi.org/10.1109/TNSRE.2022.3157446.
15. Karas, G. *et al.* (2008) 'Amnestic Mild Cognitive Impairment: Structural MR Imaging Findings Predictive of Conversion to Alzheimer Disease', *American Journal of Neuroradiology*, 29(5), pp. 944–949. Available at: https://doi.org/10.3174/ajnr.A0949.
16. Karow, D.S. *et al.* (2010) 'Relative Capability of MR Imaging and FDG PET to Depict Changes Associated with Prodromal and Early Alzheimer Disease', *Radiology*, 256(3), pp. 932–942. Available at: https://doi.org/10.1148/radiol.10091402.
17. Komosar, M., Fiedler, P. and Haueisen, J. (2022) 'Bad channel detection in EEG recordings', *Current Directions in Biomedical Engineering*, 8(2), pp. 257–260. Available at: https://doi.org/10.1515/cdbme-2022-1066.
18. Li, Y. *et al.* (2008) 'Regional analysis of FDG and PIB-PET images in normal aging, mild cognitive impairment, and Alzheimer's disease', *European Journal of Nuclear Medicine and Molecular Imaging*, 35(12), pp. 2169–2181. Available at: https://doi.org/10.1007/s00259-008-0833-y.
19. Lowry, E. *et al.* (2020) 'Path Integration Changes as a Cognitive Marker for Vascular Cognitive Impairment?—A Pilot Study', *Frontiers in Human Neuroscience*, 14, p. 131. Available at: https://doi.org/10.3389/fnhum.2020.00131.
20. May, C.P. and Hasher, L. (1998) 'Synchrony effects in inhibitory control over thought and action.', *Journal of Experimental Psychology: Human Perception and Performance*, 24(2), pp. 363–379. Available at: https://doi.org/10.1037/0096-1523.24.2.363.
21. McDonald, C.R. *et al.* (2009) 'Regional rates of neocortical atrophy from normal aging to early Alzheimer disease', *Neurology*, 73(6), pp. 457–465. Available at: https://doi.org/10.1212/WNL.0b013e3181b16431.
22. McKhann, G.M. *et al.* (2011) 'The diagnosis of dementia due to Alzheimer's disease: recommendations from the National Institute on Aging-Alzheimer's Association workgroups on diagnostic guidelines for Alzheimer's disease', *Alzheimer's & Dementia: The Journal of the Alzheimer's Association*, 7(3), pp. 263–269. Available at: https://doi.org/10.1016/j.jalz.2011.03.005.
23. Meghdadi, A.H. *et al.* (2021) 'Resting state EEG biomarkers of cognitive decline associated with Alzheimer's disease and mild cognitive impairment', *PLOS ONE*, 16(2), p. e0244180. Available at: https://doi.org/10.1371/journal.pone.0244180.
24. Merry, K. and Bettinger, P. (2019) 'Smartphone GPS accuracy study in an urban environment', *PLoS ONE*, 14(7), p. e0219890. Available at: https://doi.org/10.1371/journal.pone.0219890.
25. Monllor, P. *et al.* (2021) 'Electroencephalography as a Non-Invasive Biomarker of Alzheimer's Disease: A Forgotten Candidate to Substitute CSF Molecules?', *International Journal of Molecular Sciences*, 22(19), p. 10889. Available at: https://doi.org/10.3390/ijms221910889.
26. Morganti, F., Stefanini, S. and Riva, G. (2013) 'From allo- to egocentric spatial ability in early Alzheimer's disease: A study with virtual reality spatial tasks', *Cognitive Neuroscience*, 4(3–4), pp. 171–180. Available at: https://doi.org/10.1080/17588928.2013.854762.
27. Musaeus, C.S. *et al.* (2018) 'EEG Theta Power Is an Early Marker of Cognitive Decline in Dementia due to Alzheimer's Disease', *Journal of Alzheimer's Disease*, 64(4), pp. 1359–1371. Available at:

https://doi.org/10.3233/JAD-180300.
28. Näätänen, R. *et al.* (2014) 'Mismatch Negativity (MMN) as an Index of Cognitive Dysfunction', *Brain topography*, 27(4), pp. 451–466. Available at: https://doi.org/10.1007/s10548-014-0374-6.
29. Nestor, P.J. *et al.* (2003) 'Limbic hypometabolism in Alzheimer's disease and mild cognitive impairment', *Annals of Neurology*, 54(3), pp. 343–351. Available at: https://doi.org/10.1002/ana.10669.
30. Nobili, F. *et al.* (2008) 'Brain SPECT in subtypes of mild cognitive impairment: Findings from the DESCRIPA multicenter study', *Journal of Neurology*, 255(9), pp. 1344–1353. Available at: https://doi.org/10.1007/s00415-008-0897-4.
31. Pappatà, S. *et al.* (2010) 'SPECT imaging of GABAA/benzodiazepine receptors and cerebral perfusion in mild cognitive impairment', *European Journal of Nuclear Medicine and Molecular Imaging*, 37(6), pp. 1156–1163. Available at: https://doi.org/10.1007/s00259-010-1409-1.
32. Pennanen, C. *et al.* (2004) 'Hippocampus and entorhinal cortex in mild cognitive impairment and early AD', *Neurobiology of Aging*, 25(3), pp. 303–310. Available at: https://doi.org/10.1016/S0197-4580(03)00084-8.
33. Petersen, R.C. *et al.* (2006) 'Neuropathologic Features of Amnestic Mild Cognitive Impairment', *Archives of Neurology*, 63(5), p. 665. Available at: https://doi.org/10.1001/archneur.63.5.665.
34. Puthusseryppady, V. *et al.* (2022) 'Predicting real world spatial disorientation in Alzheimer's disease patients using virtual reality navigation tests', *Scientific Reports*, 12(1), p. 13397. Available at: https://doi.org/10.1038/s41598-022-17634-w.
35. Risacher, S.L. *et al.* (2010) 'Longitudinal MRI atrophy biomarkers: Relationship to conversion in the ADNI cohort', *Neurobiology of Aging*, 31(8), pp. 1401–1418. Available at: https://doi.org/10.1016/j.neurobiolaging.2010.04.029.
36. Scahill, R.I. *et al.* (2002) 'Mapping the evolution of regional atrophy in Alzheimer's disease: Unbiased analysis of fluid-registered serial MRI', *Proceedings of the National Academy of Sciences*, 99(7), pp. 4703–4707. Available at: https://doi.org/10.1073/pnas.052587399.
37. Schmidt-Wilcke, T. *et al.* (2009) 'Memory performance correlates with gray matter density in the ento-/perirhinal cortex and posterior hippocampus in patients with mild cognitive impairment and healthy controls — A voxel based morphometry study', *NeuroImage*, 47(4), pp. 1914–1920. Available at: https://doi.org/10.1016/j.neuroimage.2009.04.092.
38. Smailovic, U. *et al.* (2021) 'Decreased Global EEG Synchronization in Amyloid Positive Mild Cognitive Impairment and Alzheimer's Disease Patients—Relationship to APOE ε4', *Brain Sciences*, 11(10), p. 1359. Available at: https://doi.org/10.3390/brainsci11101359.
39. Smith, C.D. *et al.* (2007) 'Brain structural alterations before mild cognitive impairment', *Neurology*, 68(16), pp. 1268–1273. Available at: https://doi.org/10.1212/01.wnl.0000259542.54830.34.
40. Tu, S. *et al.* (2015) 'Lost in spatial translation – A novel tool to objectively assess spatial disorientation in Alzheimer's disease and frontotemporal dementia', *Cortex*, 67, pp. 83–94. Available at: https://doi.org/10.1016/j.cortex.2015.03.016.
41. Tu, S. *et al.* (2017) 'Egocentric versus Allocentric Spatial Memory in Behavioral Variant Frontotemporal Dementia and Alzheimer's Disease', *Journal of Alzheimer's Disease*, 59(3), pp. 883–892. Available at:

https://doi.org/10.3233/JAD-160592.
42. Vecchio, F. *et al.* (2018) 'Sustainable method for Alzheimer dementia prediction in mild cognitive impairment: Electroencephalographic connectivity and graph theory combined with apolipoprotein E', *Annals of Neurology*, 84(2), pp. 302–314. Available at: https://doi.org/10.1002/ana.25289.
43. Vecchio, F. *et al.* (2020) 'Classification of Alzheimer's Disease with Respect to Physiological Aging with Innovative EEG Biomarkers in a Machine Learning Implementation', *Journal of Alzheimer's Disease*, 75(4), pp. 1253–1261. Available at: https://doi.org/10.3233/JAD-200171.
44. Waterlander, W.E. *et al.* (2011) 'The virtual supermarket: An innovative research tool to study consumer food purchasing behaviour', *BMC Public Health*, 11(1), p. 589. Available at: https://doi.org/10.1186/1471-2458-11-589.
45. Weniger, G. *et al.* (2011) 'Egocentric and allocentric memory as assessed by virtual reality in individuals with amnestic mild cognitive impairment', *Neuropsychologia*, 49(3), pp. 518–527. Available at: https://doi.org/10.1016/j.neuropsychologia.2010.12.031.
46. Whitwell, J.L. *et al.* (2008) 'MRI patterns of atrophy associated with progression to AD in amnestic mild cognitive impairment', *Neurology*, 70(7), pp. 512–520. Available at: https://doi.org/10.1212/01.wnl.0000280575.77437.a2.
47. Wolbers, T. *et al.* (2008) 'Spatial updating: how the brain keeps track of changing object locations during observer motion', *Nature Neuroscience*, 11(10), pp. 1223–1230. Available at: https://doi.org/10.1038/nn.2189.
48. Wolbers, T., Weiller, C. and Büchel, C. (2004) 'Neural foundations of emerging route knowledge in complex spatial environments', *Cognitive Brain Research*, 21(3), pp. 401–411. Available at: https://doi.org/10.1016/j.cogbrainres.2004.06.013.
49. Zandbergen, P.A. and Barbeau, S.J. (2011) 'Positional Accuracy of Assisted GPS Data from High-Sensitivity GPS-enabled Mobile Phones', *The Journal of Navigation*, 64(3), pp. 381–399. Available at: https://doi.org/10.1017/S0373463311000051.